Wave-CAIPI: Highly Accelerated 3D Imaging with Reduced g-factor Penalty

B. Bilgic[1,2], B. A. Gagoski[2,3], S.F. Cauley[1,2], A.P. Fan[1,4], J.R. Polimeni[1,2], P.E. Grant[2,3], L.L.Wald[1,2,5], K. Setsompop[1,2]

1 Martinos Center for Biomedical Imaging, Charlestown, MA,
2 Harvard Medical School, Boston, MA
3 Boston Children's Hospital, Boston, MA
4 Department of Electrical Engineering and Computer Science, MIT, Cambridge, MA
5 Harvard-MIT Division of Health Sciences and Technology, MIT, Cambridge, MA

June 12, 2014

Introduction

- Recent modifications to rectilinear k-space sampling have provided more robust reconstructions of highly under-sampled datasets.

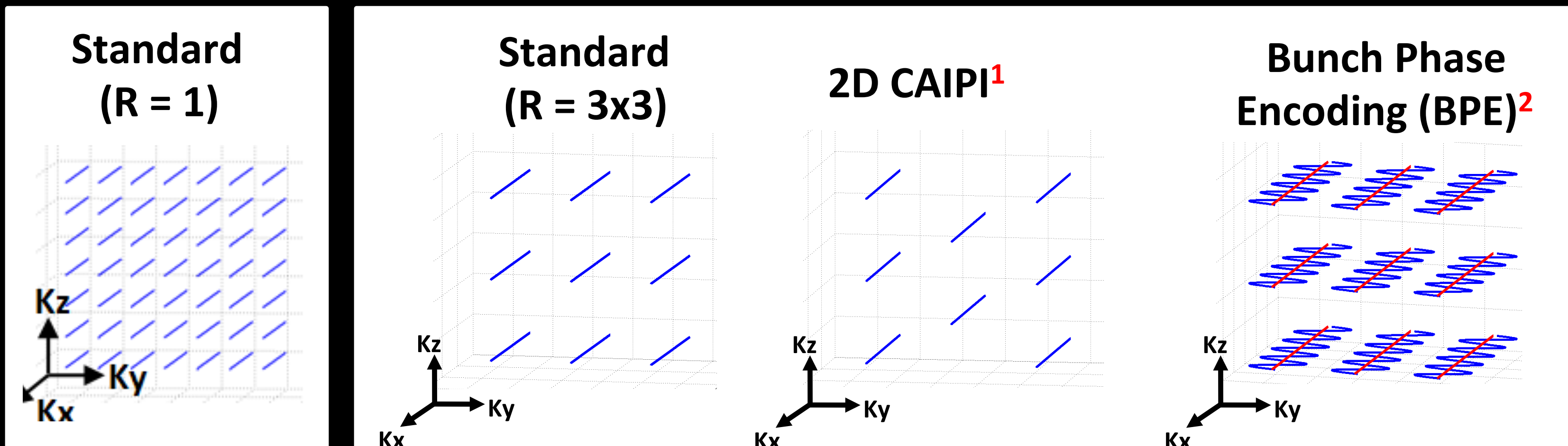

1. Breuer FA. et al, MRM 2006:55:549 2. Moriguchi H et al, MRM 2006:55:633

Introduction

- Recent modifications to rectilinear k-space sampling have provided more robust reconstructions of highly under-sampled datasets.

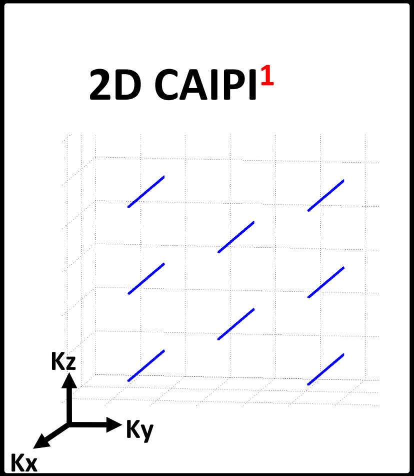

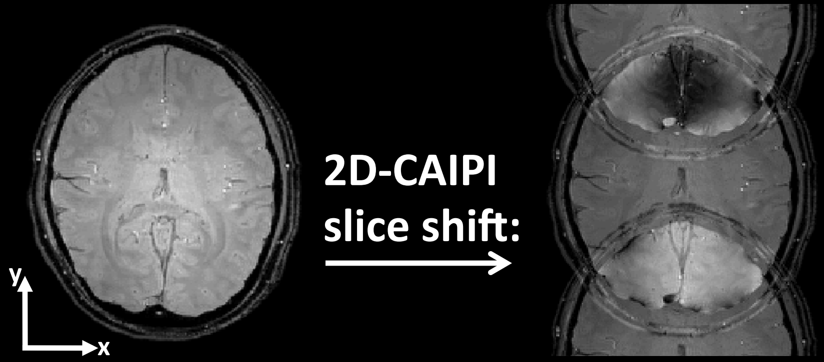

1. Breuer FA. et al, MRM 2006:55:549 2. Moriguchi H et al, MRM 2006:55:633

Introduction

- Recent modifications to rectilinear k-space sampling have provided more robust reconstructions of highly under-sampled datasets.

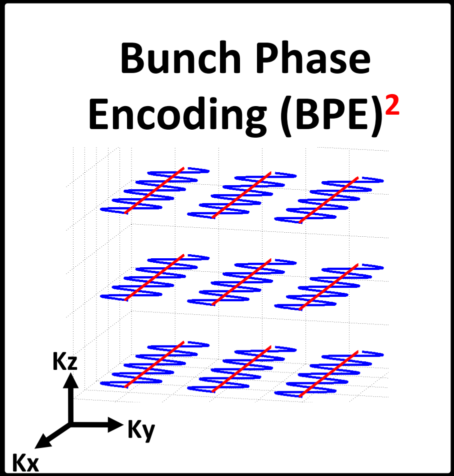

1. Breuer FA. et al, MRM 2006:55:549 2. Moriguchi H et al, MRM 2006:55:633

Introduction

- Recent modifications to rectilinear k-space sampling have provided more robust reconstructions of highly under-sampled datasets.

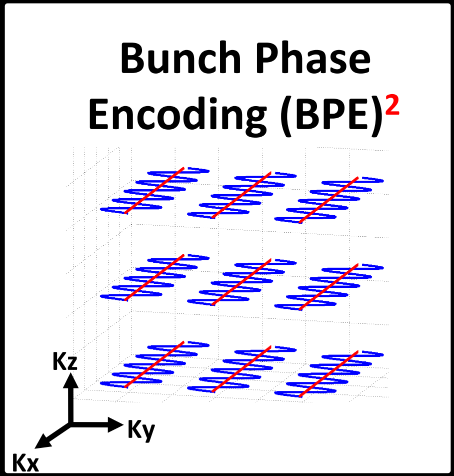

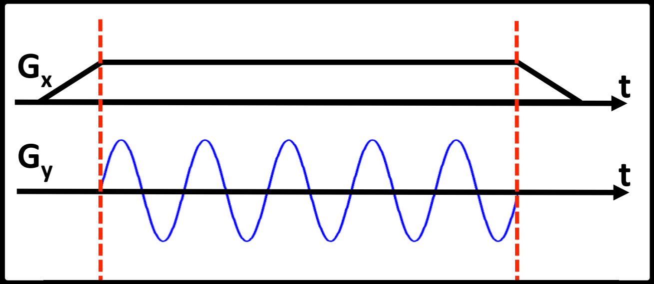

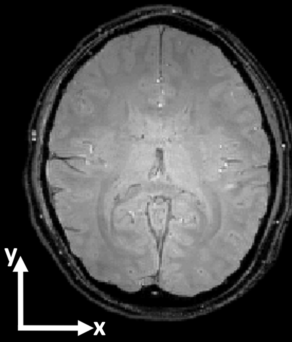

Bunch Phase: Zigzag G_y →

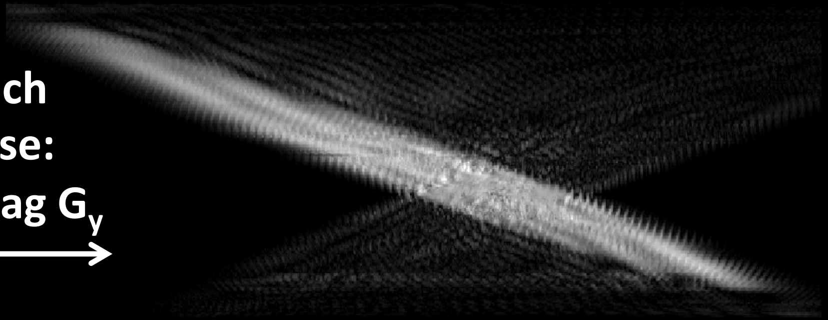

1. Breuer FA. et al, MRM 2006:55:549 2. Moriguchi H et al, MRM 2006:55:633

Introduction

- Recent modifications to rectilinear k-space sampling have provided more robust reconstructions of highly under-sampled datasets.

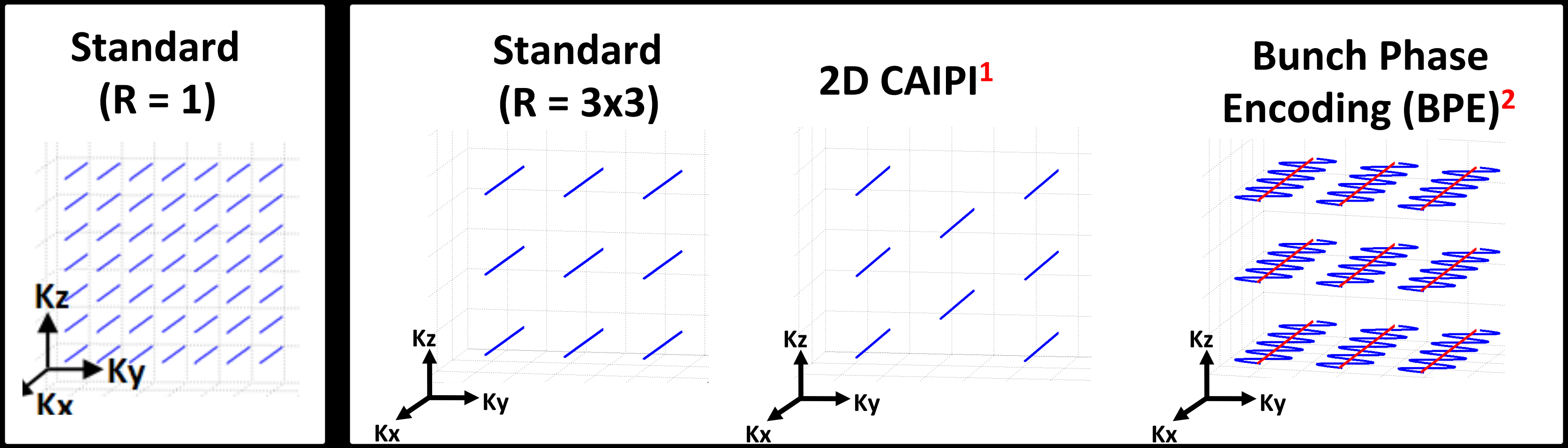

- Wave-CAIPI: 2D CAIPI + BPE in 2 direction
  - Spread aliasing in 3D to take full advantage of 3D coil profiles

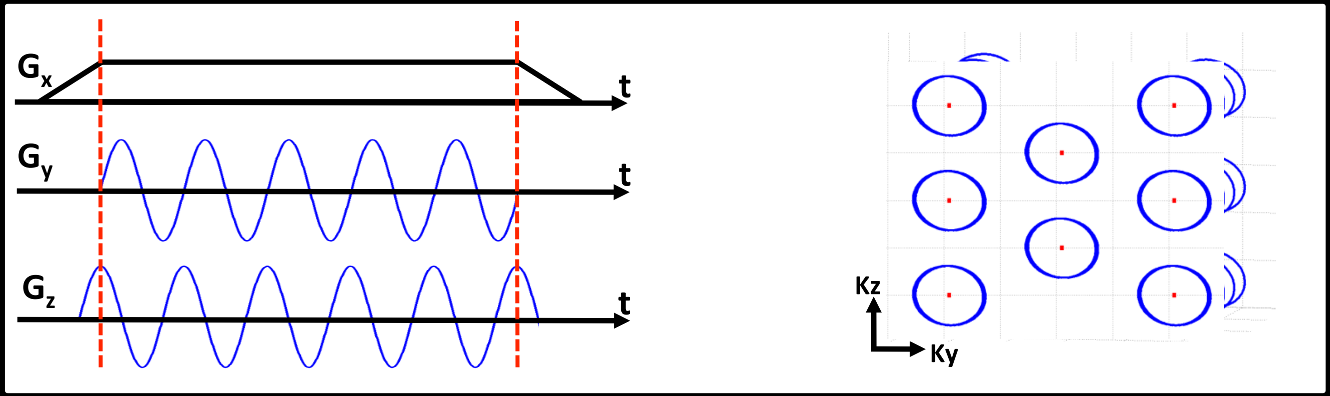

1. Breuer FA. et al, MRM 2006:55:549 2. Moriguchi H et al, MRM 2006:55:633

Effect of Wave Gradients

- Combination of G_y and G_z gradients with interslice shifts yield voxel spreading across three dimensions

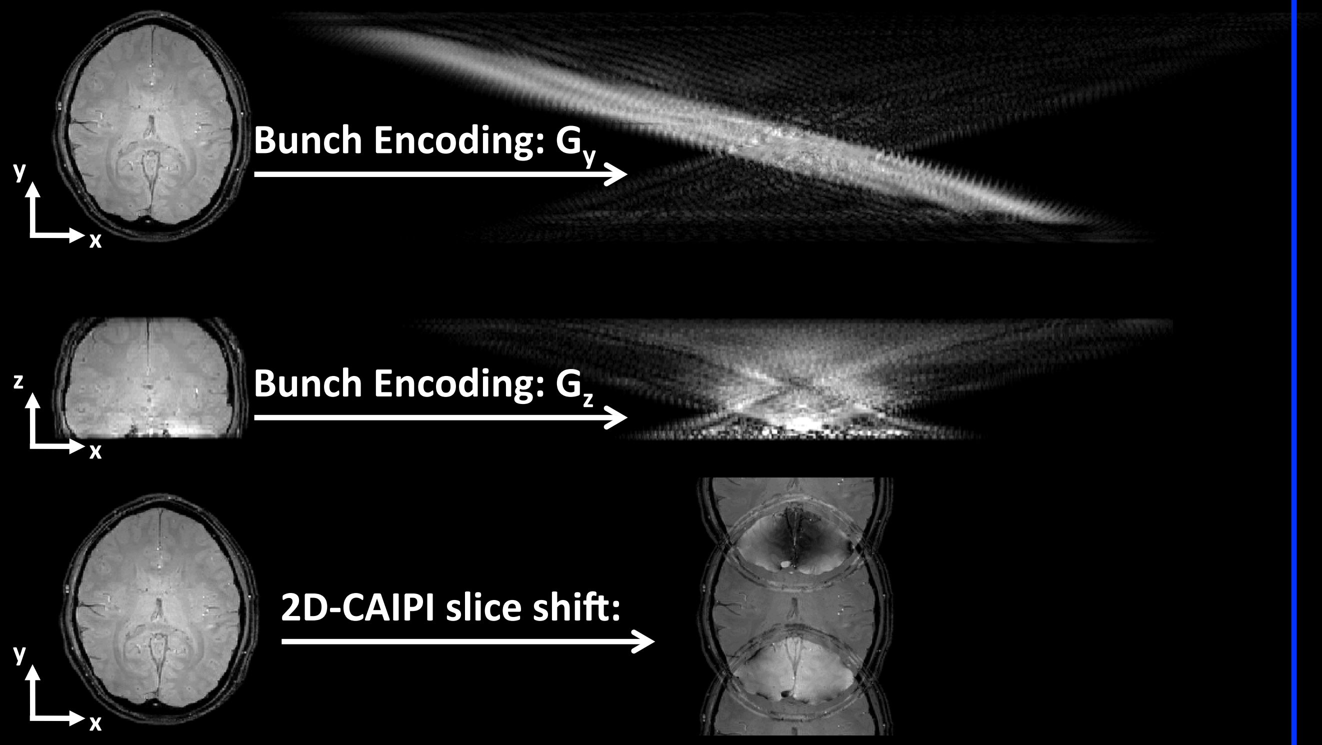

Effect of Wave Gradients

- Combination of G_y and G_z gradients with interslice shifts yield voxel spreading across three dimensions

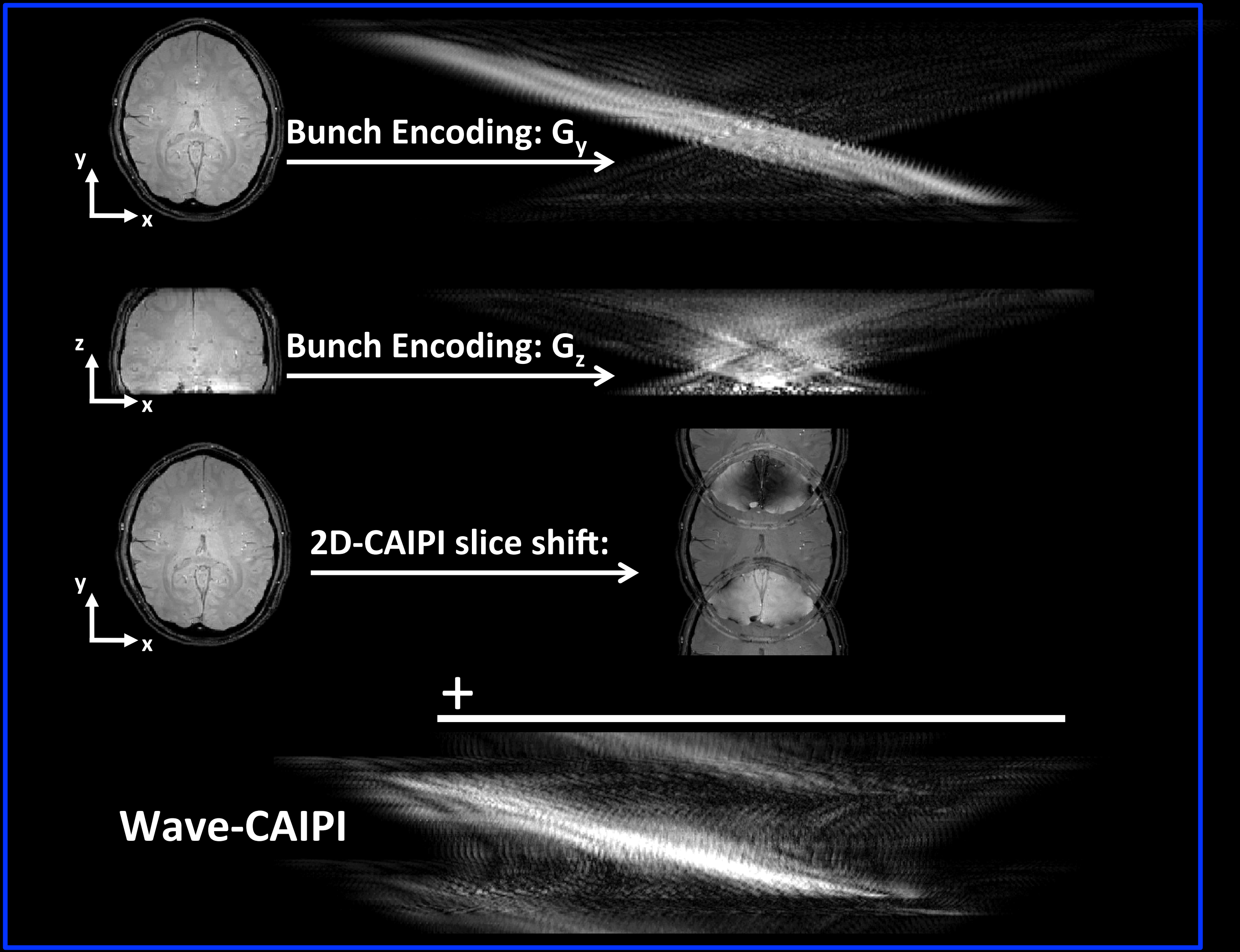

Effect of Wave Gradients

- Combination of G_y and G_z gradients with interslice shifts yield voxel spreading across three dimensions

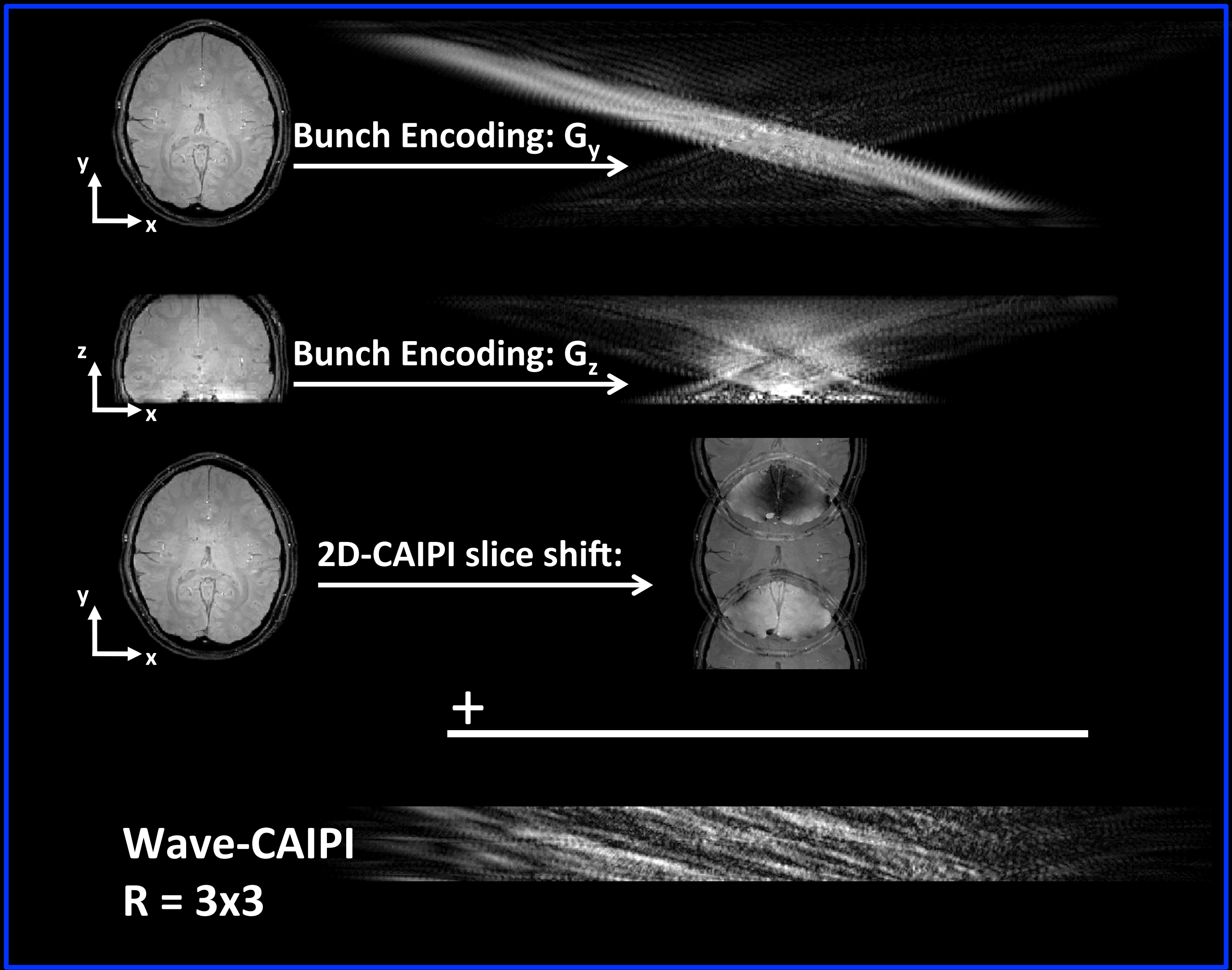

Point Spread Function

- **Wave-CAIPI = BPE G_y + BPE G_z + CAIPI 2D**
- **View BPE G_y as <u>extra modulation</u> rather than modifying k-space traj.**

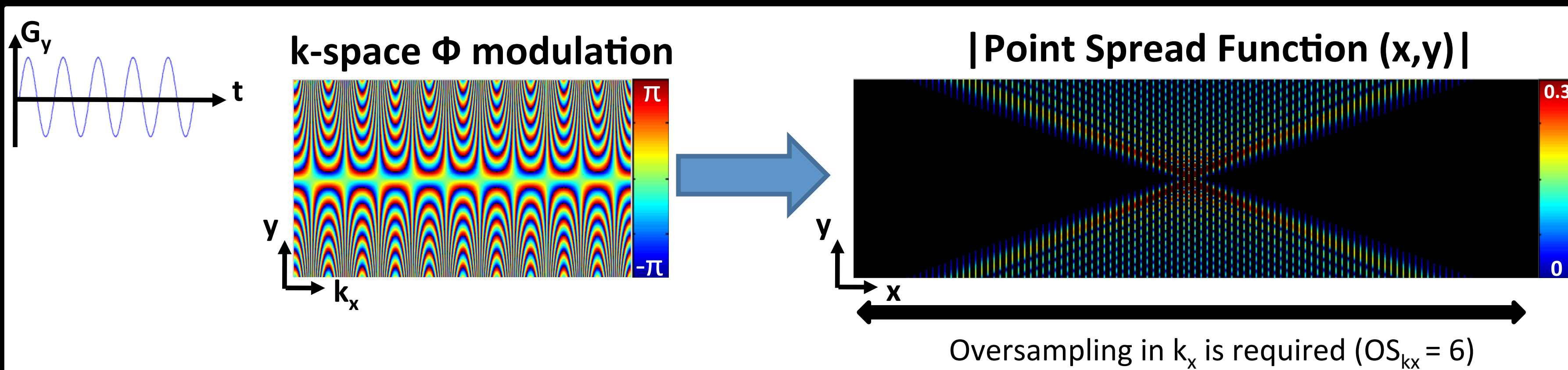

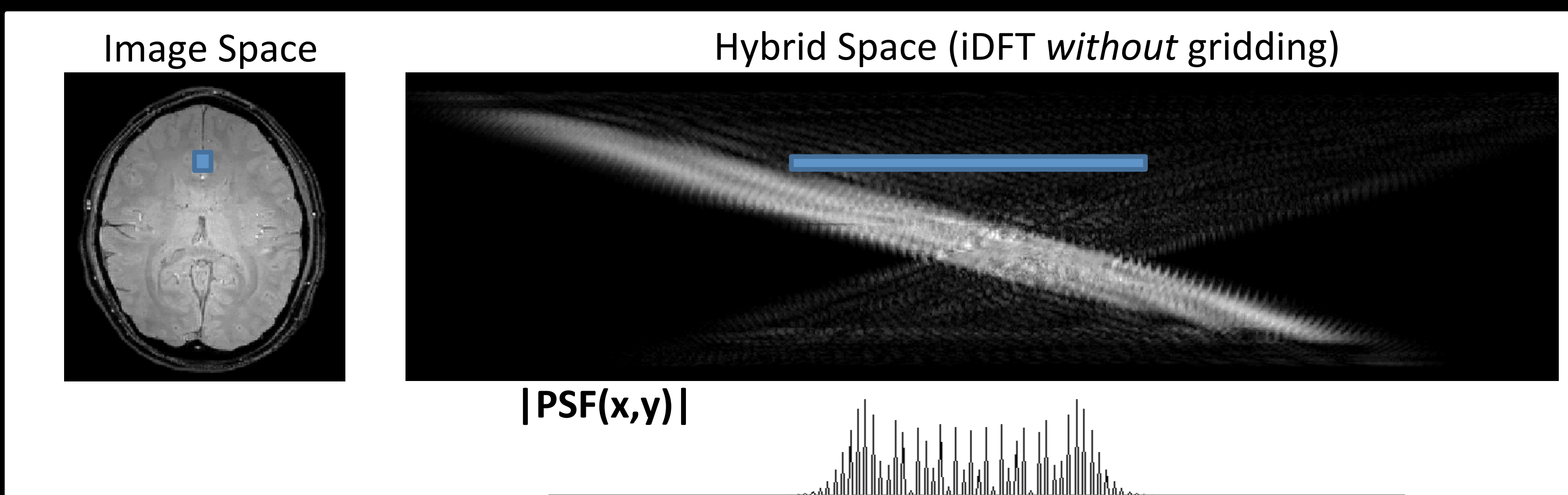

Point Spread Function

- **From signal equation:**

$$wave(x,y,z) = \sum_{k_x} e^{i2\pi x k_x/N} \cdot e^{-i2\pi W_y(k_x)y} \cdot \sum_{x} e^{-i2\pi x k_x/N} \cdot img(x,y,z)$$

$wave(x,y,z)$	Wave image
$img(x,y,z)$	Underlying magnetization
$W_y(k_x(t)) = \frac{\gamma}{2\pi}\int_0^t G_y(\tau)\,d\tau$	k-space trajectory

Image Space

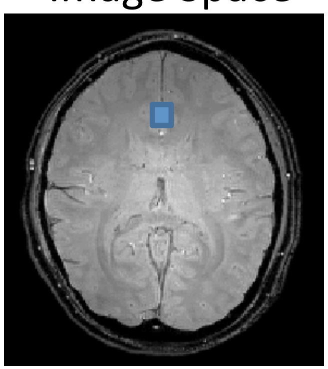

$img(x,y,z)$

Hybrid Space (iDFT *without* gridding)

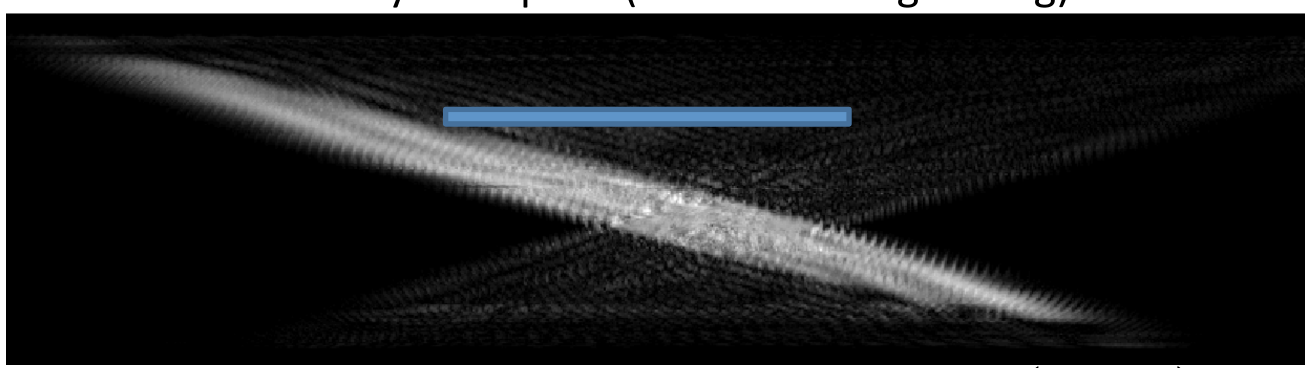

$wave(x,y,z)$

|PSF(x,y)|

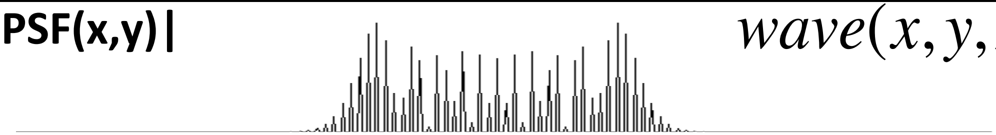

Point Spread Function

- **From signal equation:**

$$wave(x,y,z) = \underbrace{\sum_{k_x} e^{i2\pi x k_x/N}}_{\text{Inverse Discrete Fourier Transform}} \cdot e^{-i2\pi W_y(k_x)y} \cdot \underbrace{\sum_{x} e^{-i2\pi x k_x/N}}_{\text{Discrete Fourier Transform}} \cdot img(x,y,z)$$

Image Space

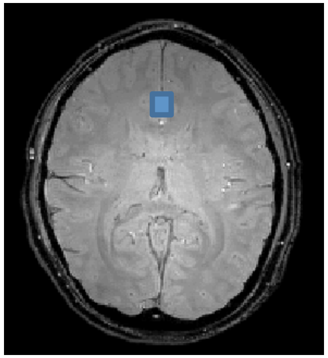

$img(x,y,z)$

Hybrid Space (iDFT *without* gridding)

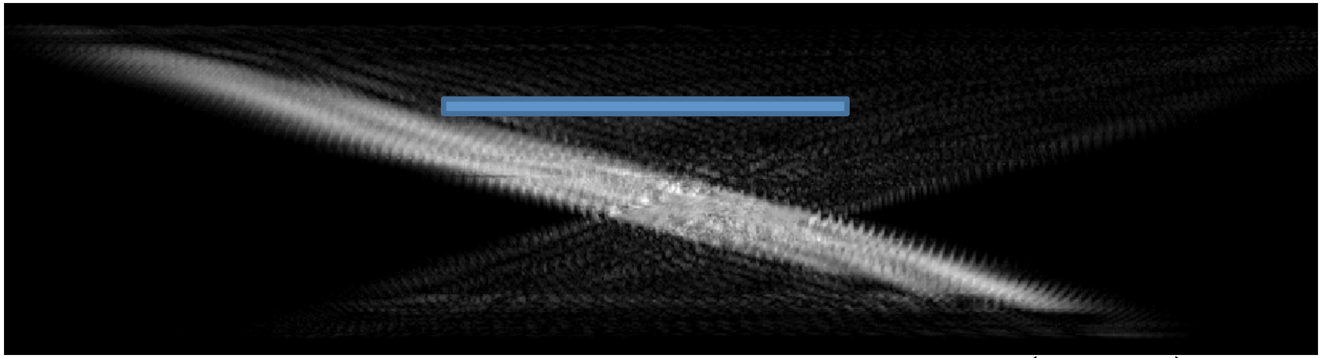

$wave(x,y,z)$

|PSF(x,y)|

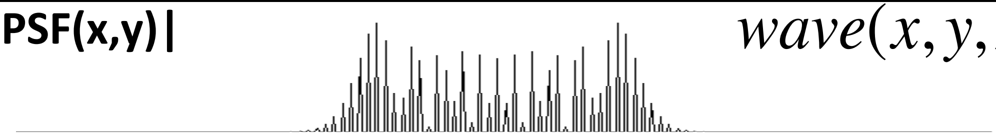

Point Spread Function

- **From signal equation:**

$$wave(x,y,z) = \mathrm{F}^{-1} \cdot \underbrace{e^{-i2\pi W_y(k_x)y}}_{\text{Point Spread Function (PSF)}} \cdot \mathrm{F} \cdot img(x,y,z)$$

No need for gridding, simple DFT

PSF(k_x,y)

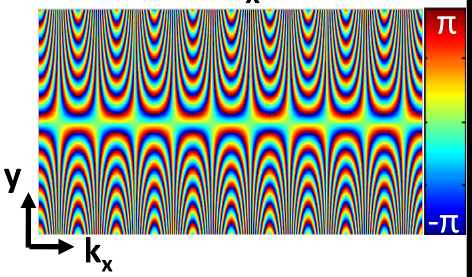

Image Space

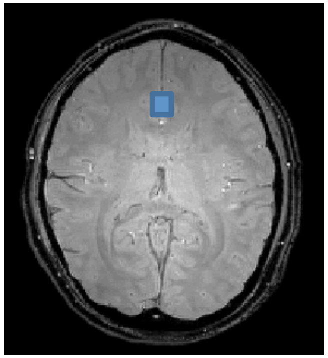

$img(x,y,z)$

Hybrid Space (iDFT *without* gridding)

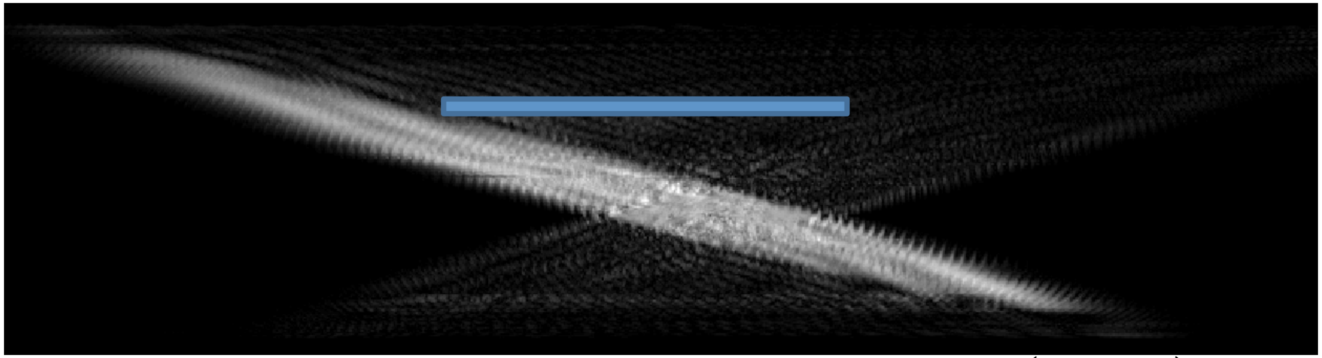

$wave(x,y,z)$

|PSF(x,y)|

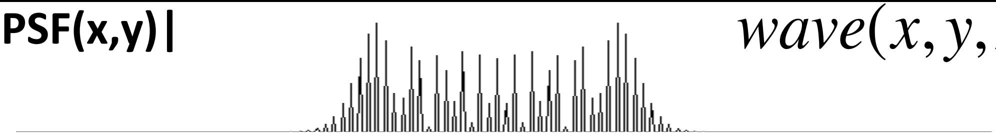

Reconstruction for accelerated acquisitions

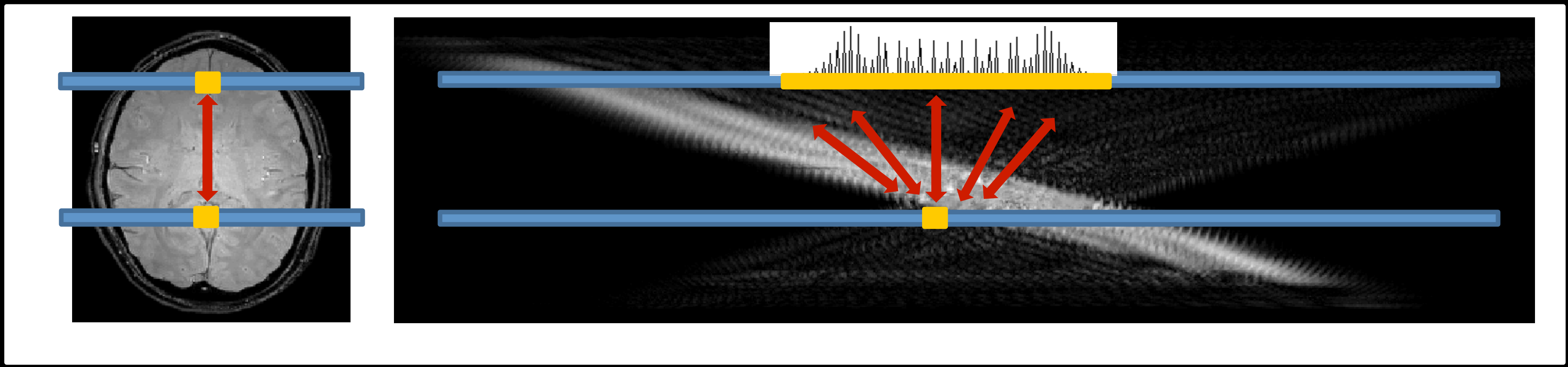

- $R_{inplane}$ = 2 => pair-wise aliasing of two rows of voxels
  => small Encoding matrix for each pair
  => separable and easy to solve
  => intuition on why Wave improves reconstruction

Reconstruction for accelerated acquisitions

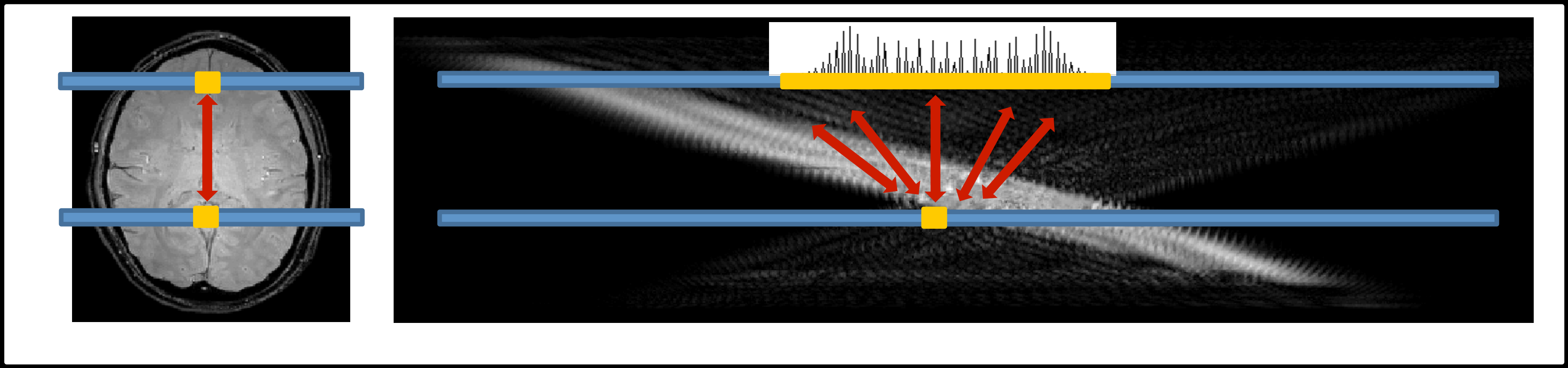

- $R_{inplane} = 2$ => pair-wise aliasing of two rows of voxels
  => small Encoding matrix for each pair
  => separable and easy to solve
  => intuition on why Wave improves reconstruction

$$wave(x,y,z) = \mathrm{F}^{-1} \cdot \underbrace{\mathrm{e}^{-i2\pi W_y(k_x)y}}_{\mathrm{Psf}(y)} \cdot \mathrm{F} \cdot img(x,y,z)$$

Reconstruction for accelerated acquisitions

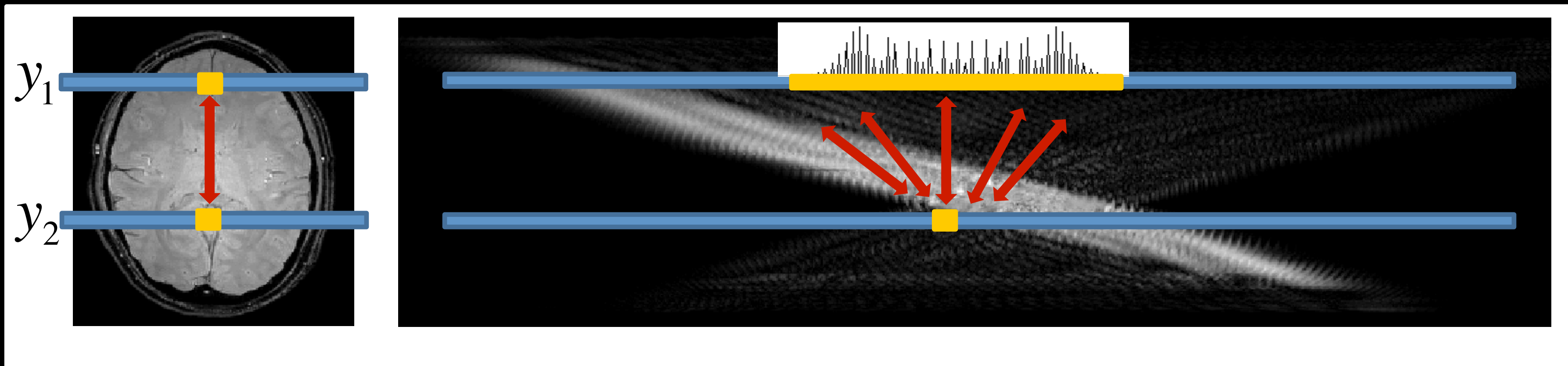

- $R_{inplane} = 2$ => pair-wise aliasing of two rows of voxels
  => small Encoding matrix for each pair
  => separable and easy to solve
  => intuition on why Wave improves reconstruction

$$wave(y) = \mathrm{F}^{-1} \cdot \mathrm{Psf}(y) \cdot \mathrm{F} \cdot row(y)$$

$$\begin{bmatrix} \mathrm{F}^{-1} \cdot \mathrm{Psf}(y_1) \cdot \mathrm{F} \\ \mathrm{F}^{-1} \cdot \mathrm{Psf}(y_2) \cdot \mathrm{F} \end{bmatrix} \cdot \begin{bmatrix} row(y_1) \\ row(y_2) \end{bmatrix} = \begin{bmatrix} wave \end{bmatrix}$$

Reconstruction for accelerated acquisitions

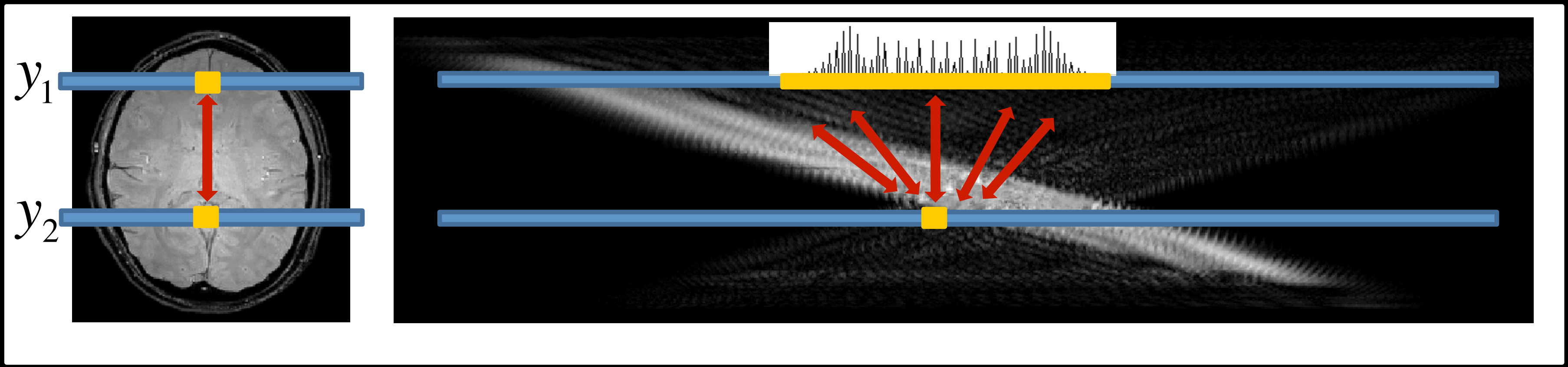

- $R_{inplane} = 2$ => pair-wise aliasing of two rows of voxels
  => <u>small</u> Encoding matrix for each pair
  => separable and easy to solve
  => intuition on why Wave improves reconstruction

$$wave(y) = \mathrm{F}^{-1} \cdot \mathrm{Psf}(y) \cdot \mathrm{F} \cdot row(y)$$

$$\begin{bmatrix} \mathrm{F}^{-1} \cdot \mathrm{Psf}(y_1) \cdot \mathrm{F} \cdot \mathrm{C}(y_1) \\ \mathrm{F}^{-1} \cdot \mathrm{Psf}(y_2) \cdot \mathrm{F} \cdot \mathrm{C}(y_2) \end{bmatrix} \cdot \begin{bmatrix} row(y_1) \\ row(y_2) \end{bmatrix} = \begin{bmatrix} wave \end{bmatrix}$$

Reconstruction for accelerated acquisitions

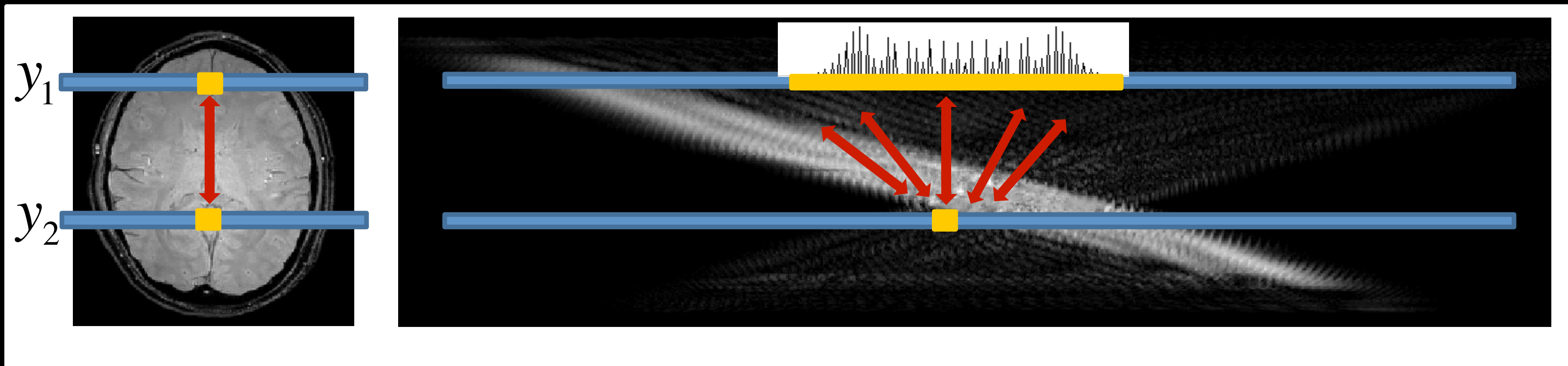

- $R_{inplane} = 2$ => pair-wise aliasing of two rows of voxels
  => <u>small</u> Encoding matrix for each pair
  => separable and easy to solve
  => intuition on why Wave improves reconstruction

$$wave(y) = F^{-1} \cdot Psf(y) \cdot F \cdot row(y)$$

$$\underbrace{\begin{bmatrix} F^{-1} \cdot Psf(y_1) \cdot F \cdot C_1(y_1) \\ \cdots \\ F^{-1} \cdot Psf(y_2) \cdot F \cdot C_{32}(y_2) \end{bmatrix}}_{\text{Encoding matrix}} \cdot \begin{bmatrix} row(y_1) \\ row(y_2) \end{bmatrix} = \begin{bmatrix} wave_1 \\ \cdots \\ wave_{32} \end{bmatrix}$$

Reconstruction for accelerated acquisitions

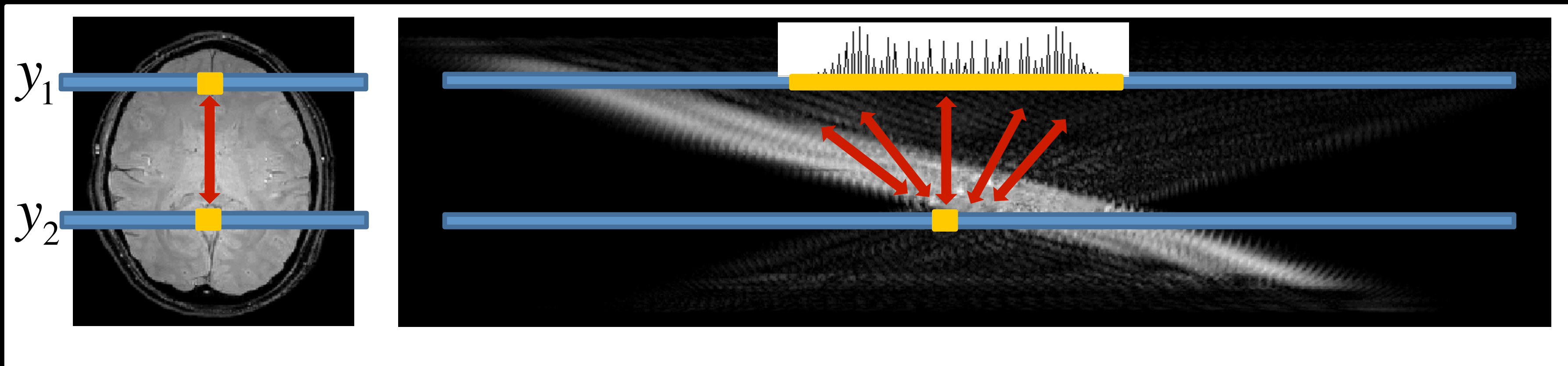

- $R_{inplane} = 2$ => pair-wise aliasing of two rows of voxels
  - => small Encoding matrix for each pair
  - => separable and easy to solve
  - => intuition on why Wave improves reconstruction

$$wave(y) = F^{-1} \cdot Psf(y) \cdot F \cdot row(y)$$

$$\begin{bmatrix} F^{-1} \cdot Psf(y_1) \cdot F \cdot C_1(y_1) \\ \dots \\ F^{-1} \cdot Psf(y_2) \cdot F \cdot C_{32}(y_2) \end{bmatrix} \cdot \begin{bmatrix} row(y_1) \\ row(y_2) \end{bmatrix} = \begin{bmatrix} wave_1 \\ \dots \\ wave_{32} \end{bmatrix}$$

- Solve for each set of collapsed rows iteratively using LSQR

Wave-CAIPI reconstruction

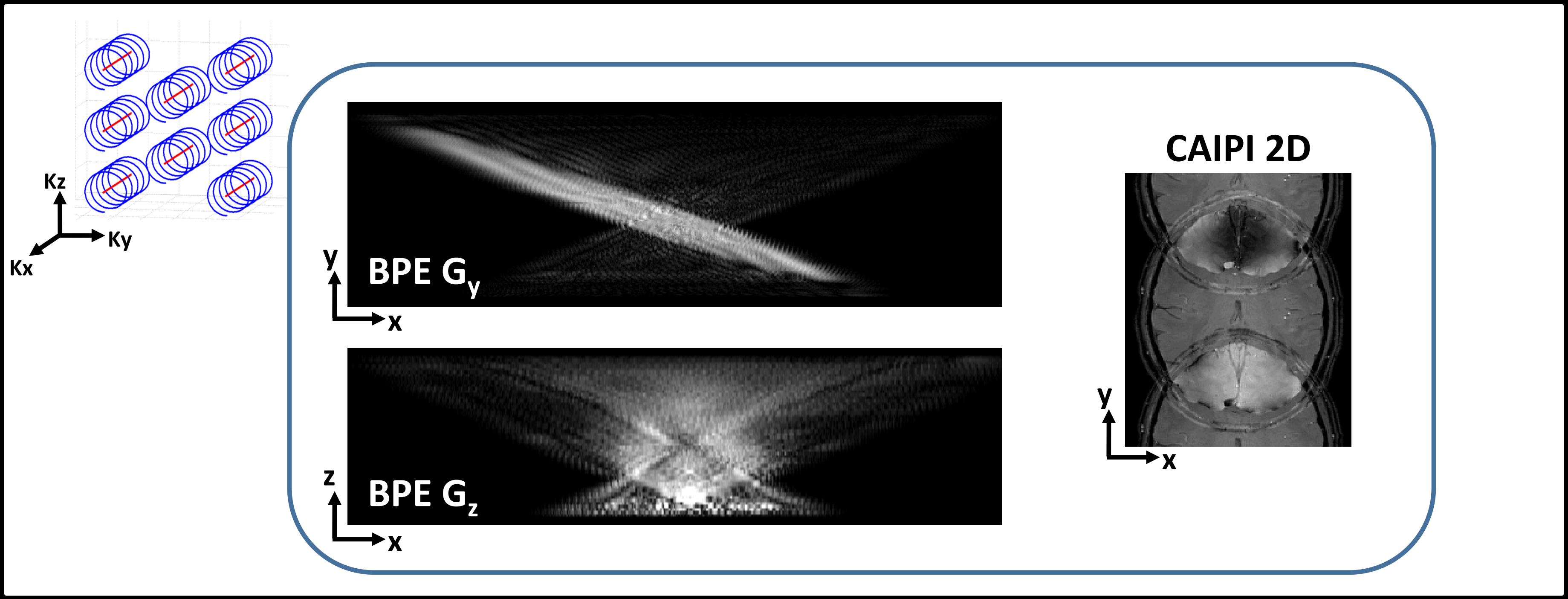

⇒ Wave gradients G_y and G_z create position dependent PSF

⇒ CAIPI 2D shift aliasing pattern

⇒ These are accounted for when generating the PSF-based Encoding matrices

- ⇒ Ex: R = 3x3
  - ⇒ each Encoding matrix corresponds to 9 rows of the image
  - ⇒ grouping of rows is determined by CAIPI 2D
  - ⇒ amount of spreading in each row determined by G_y and G_z

Artifact Quantification

PSF over image FOV_y

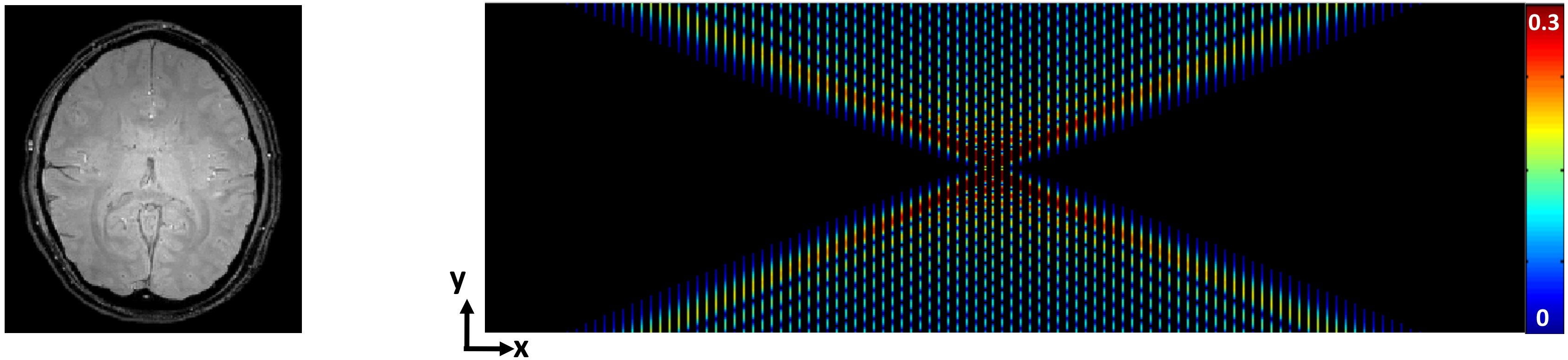

How about PSF over a voxel?

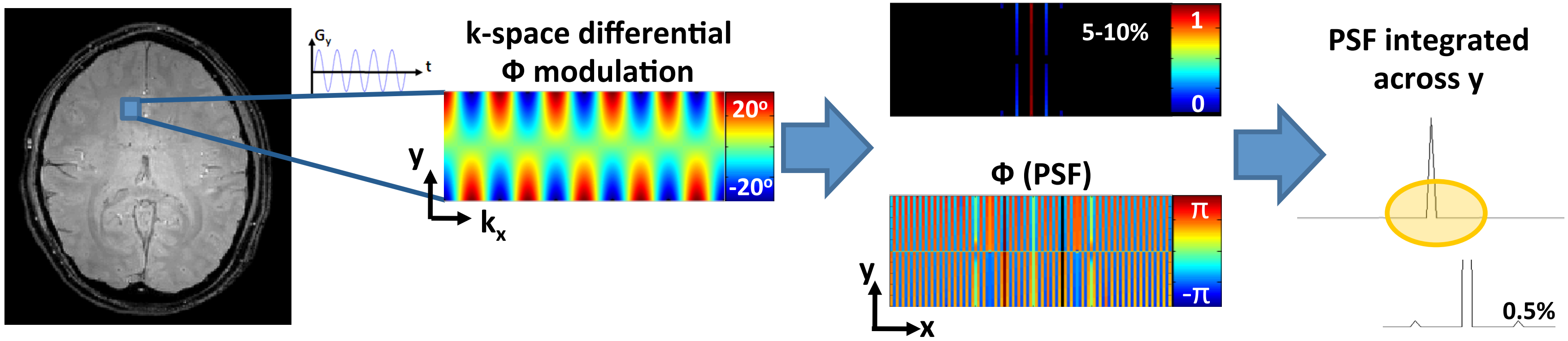

In Vivo Acquisition Comparison

- Compare Wave-CAIPI and conventional SENSE
- Acquire **fully-sampled** data, then accelerate by R = 3x3
- Compute root-mean-square error (RMSE) and 1/g-factor maps (retained SNR)

In Vivo Acquisition Comparison

- Compare Wave-CAIPI and conventional SENSE
- Acquire **fully-sampled** data, then accelerate by R = 3x3
- Compute root-mean-square error (RMSE) and 1/g-factor maps (retained SNR)
- In vivo acquisitions:
  - At 3T and 7T
  - 1x1x2 mm resolution
  - 224x224x120 FOV

3 Tesla, R=3x3, 1x1x2 mm^3, T_{acq}=38s

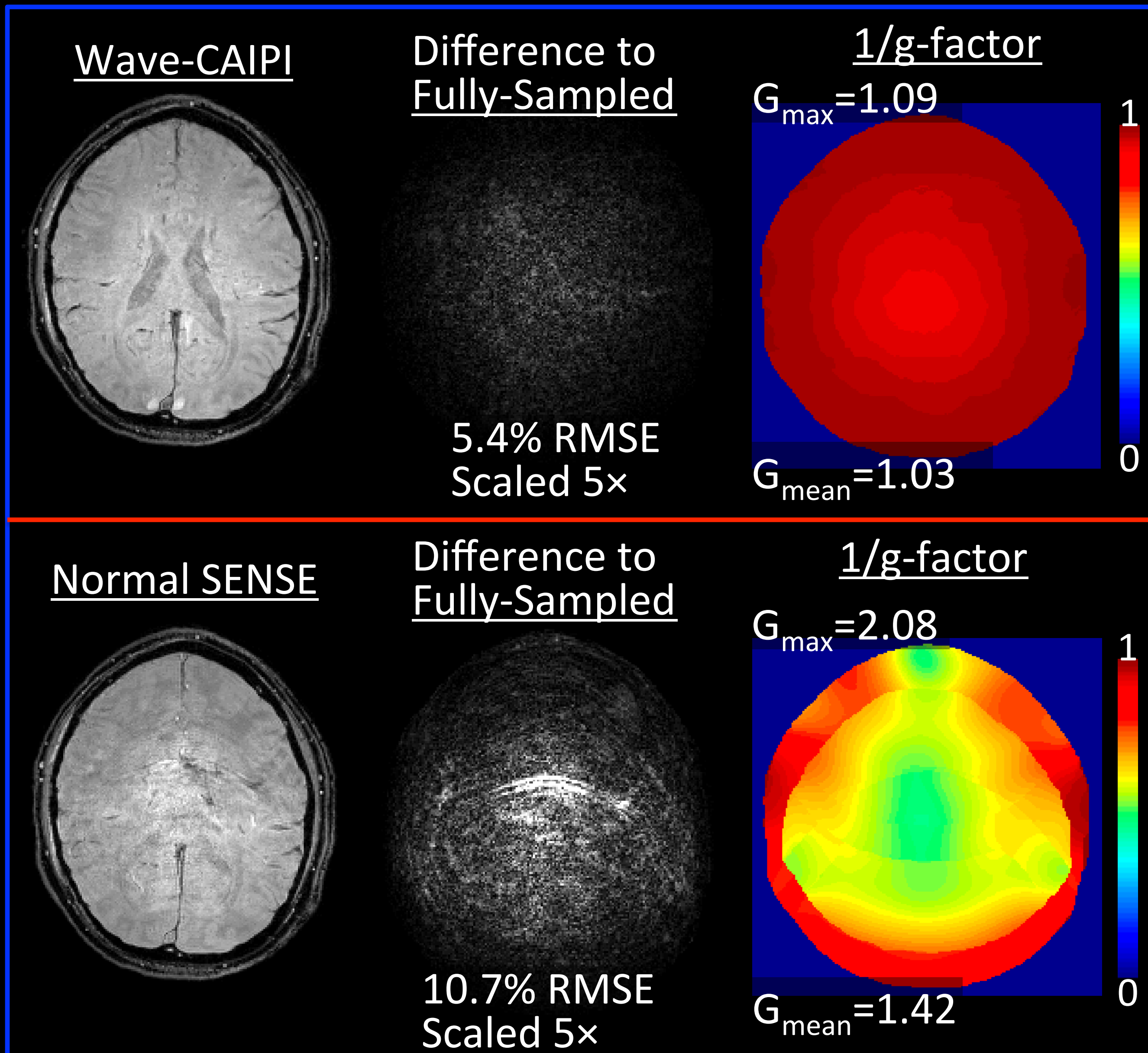

TR/TE = 26/13.3 ms

7 Tesla, R=3x3, 1x1x2 mm^3, T_{acq}=40s

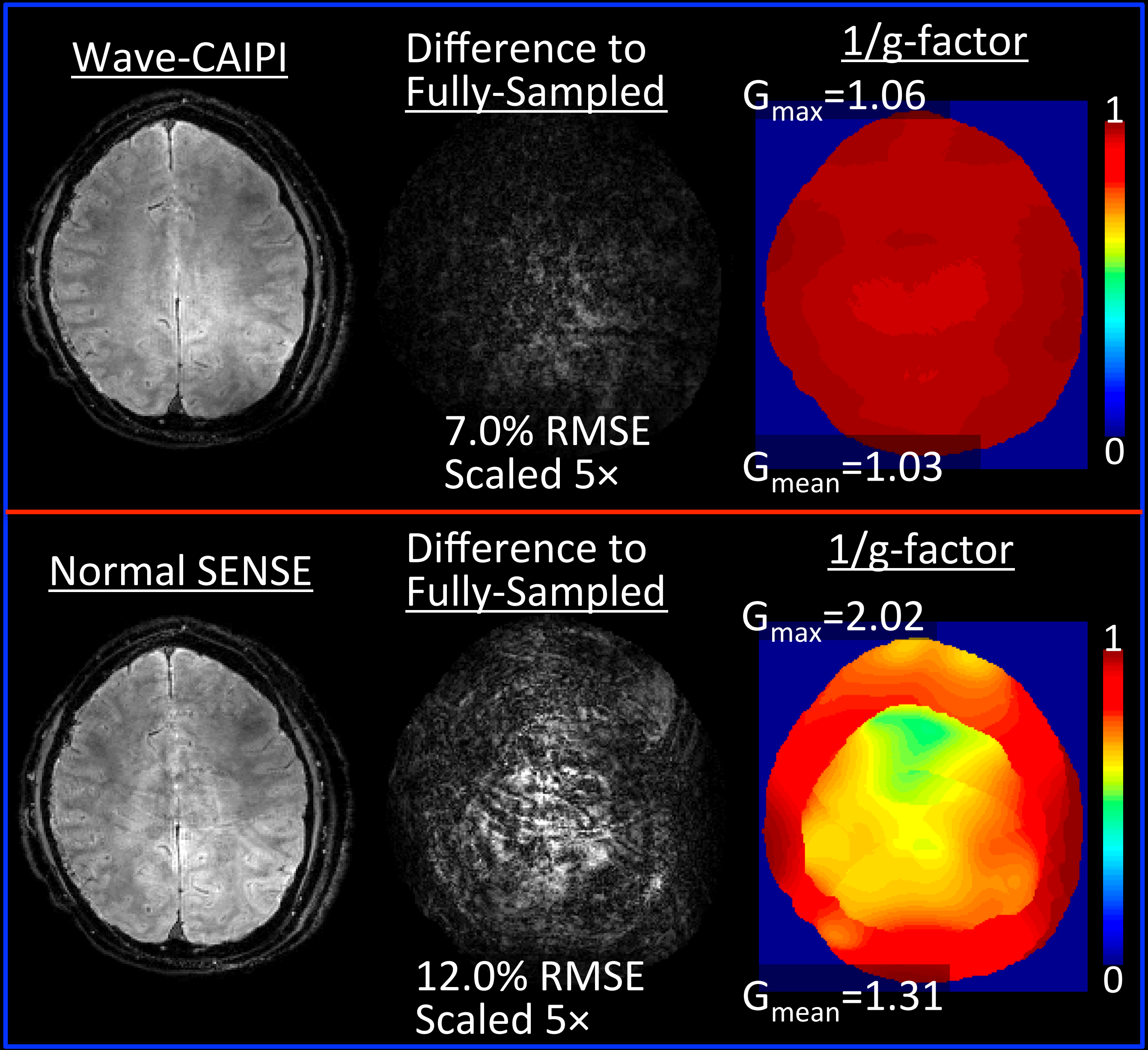

TR/TE = 27/10.9 ms

Accelerated Acquisition Comparison

- Compare Wave-CAIPI, 2D-CAIPI[1] and Bunch Phase[2]
- Acquire R = 3x3 accelerated data
- Compute 1/g-factor maps (retained SNR)

1. Breuer FA. et al, MRM 2006:55:549 2. Moriguchi H et al, MRM 2006:55:633

Accelerated Acquisition Comparison

- Compare Wave-CAIPI, 2D-CAIPI[1] and Bunch Phase[2]
- Acquire R = 3x3 accelerated data
- Compute 1/g-factor maps (retained SNR)
- In vivo acquisitions:
  - At 3T and 7T
  - 1x1x1 mm isotropic resolution
  - Acquisition time: 2.3 min
  - 240x240x120 FOV

1. Breuer FA. et al, MRM 2006:55:549 2. Moriguchi H et al, MRM 2006:55:633

3 Tesla, R=3x3, 1x1x1 mm^3, T_{acq}=2.3 min

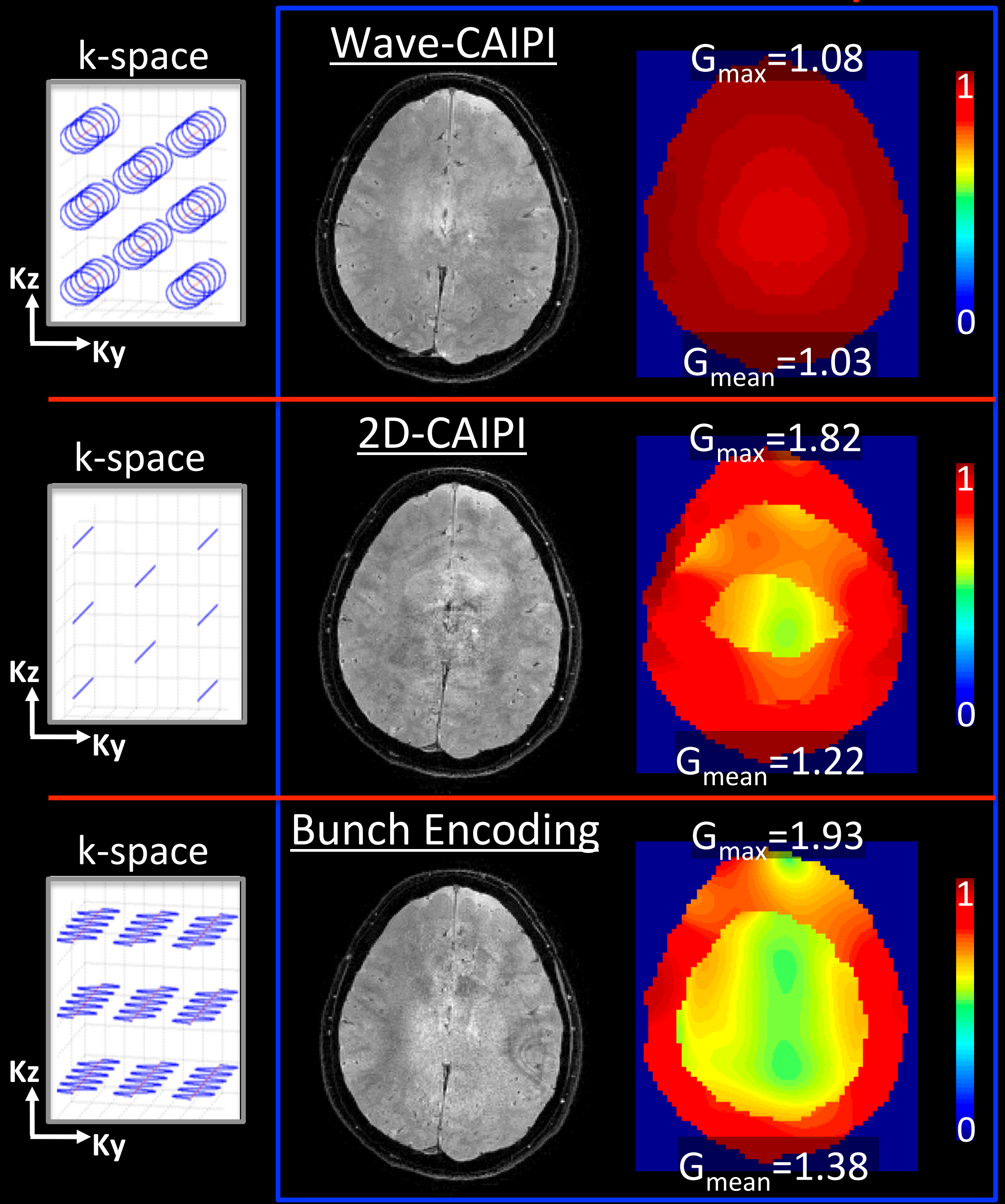

7 Tesla, R=3x3, 1x1x1 mm^3, T_{acq}=2.3 min

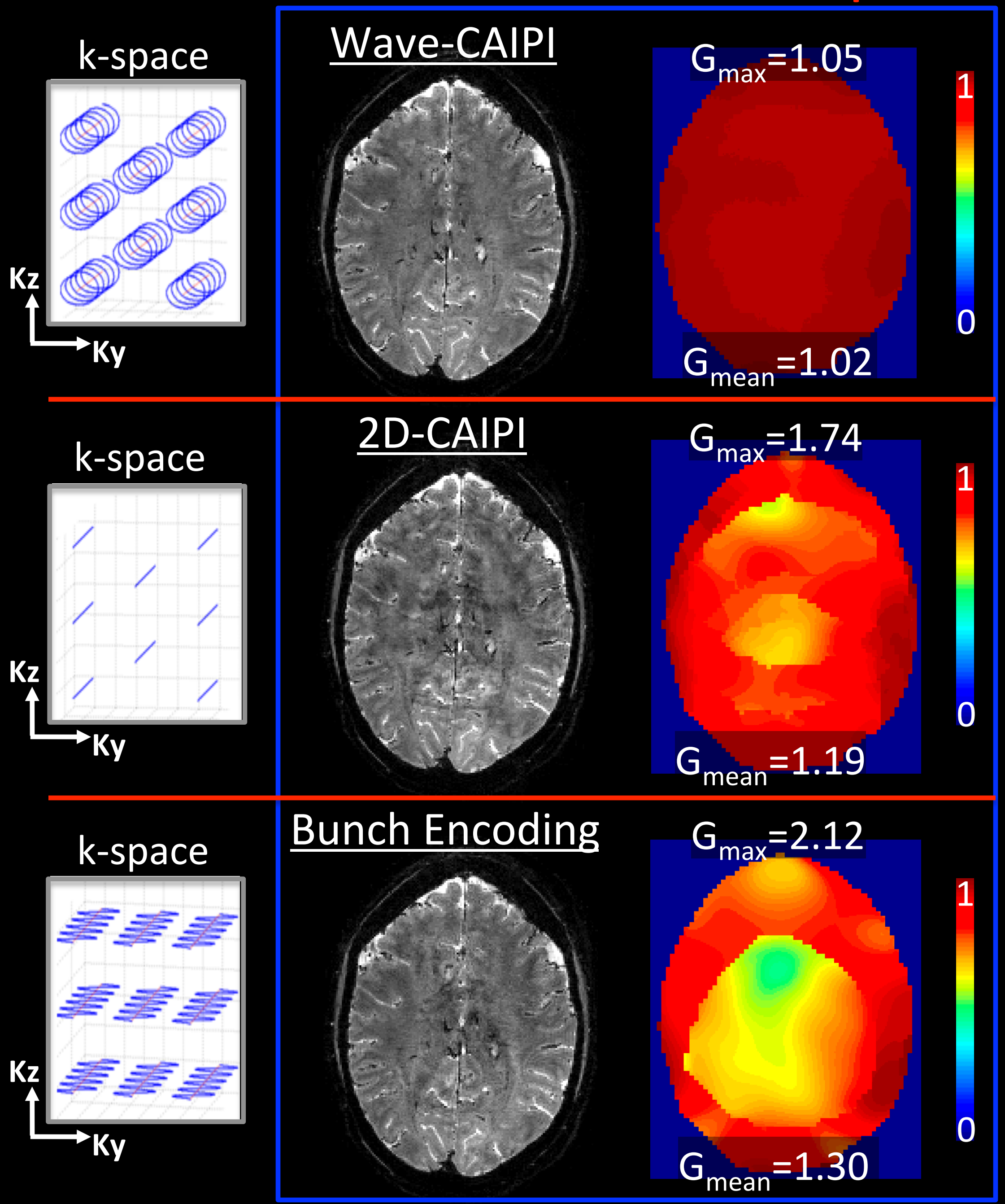

Susceptibility of Tissue

- Susceptibility χ : degree of magnetization of a material when placed in a magnetic field

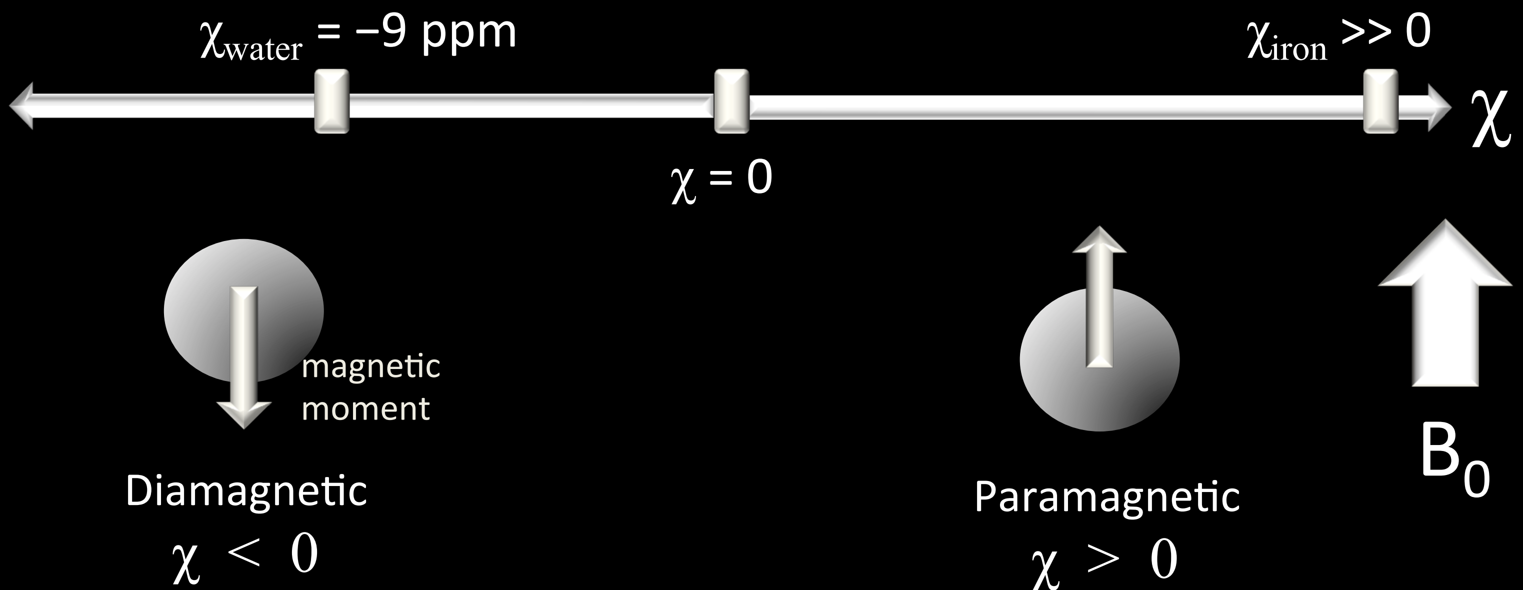

Susceptibility of Tissue

- Susceptibility χ : degree of magnetization of a material when placed in a magnetic field

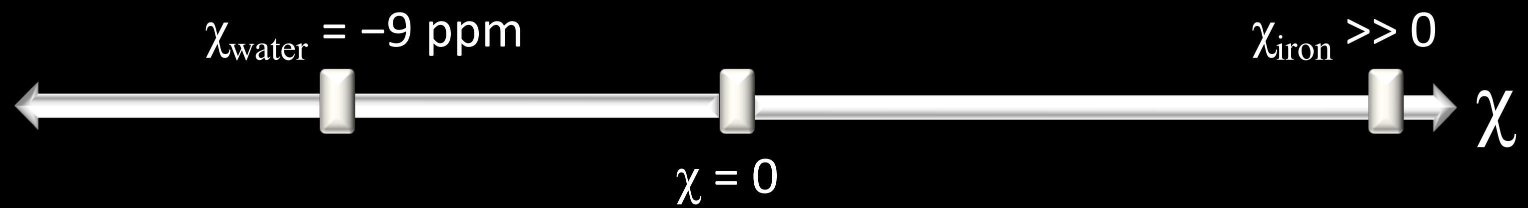

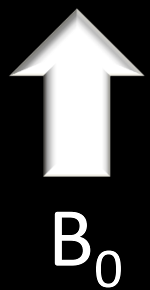

- Susceptibility of brain tissue is ≈ −9 ppm
- Tissues with increased iron deposition are relatively paramagnetic → **χ is more positive**

Susceptibility of Tissue

- Susceptibility χ : degree of magnetization of a material when placed in a magnetic field

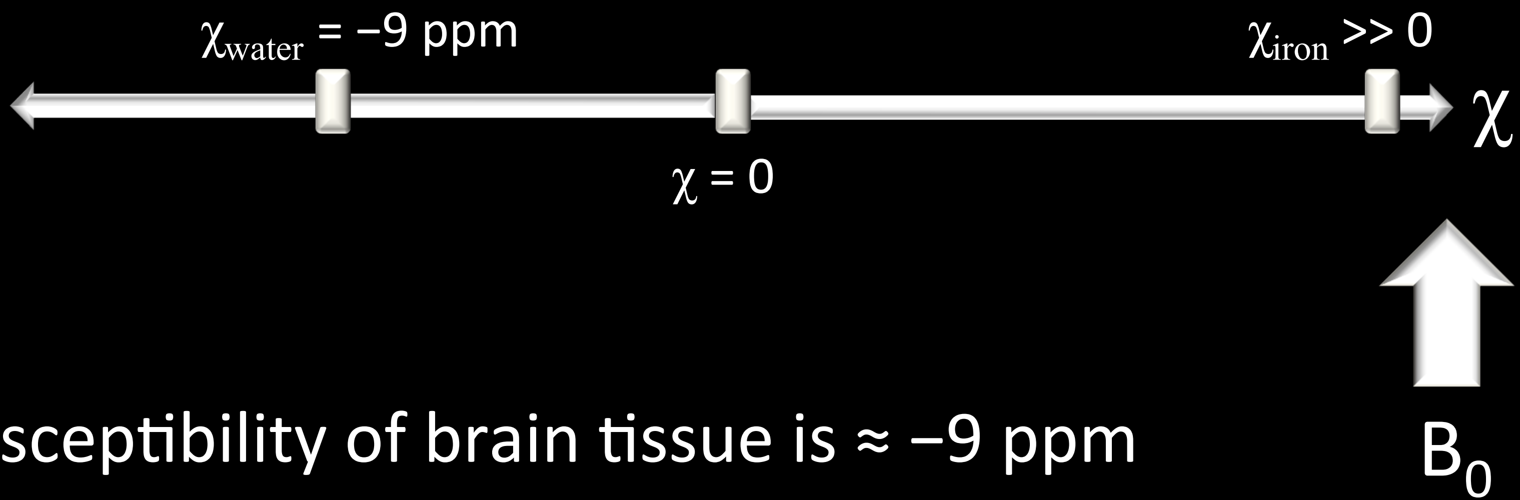

- Susceptibility of brain tissue is ≈ −9 ppm
- Tissues with increased iron deposition are relatively paramagnetic → **χ is more positive**
- Excessive iron concentration occurs in a variety of degenerative diseases,

  e.g. Alzheimer's, multiple sclerosis, Parkinson's

Susceptibility of Tissue

- Susceptibility χ : degree of magnetization of a material when placed in a magnetic field

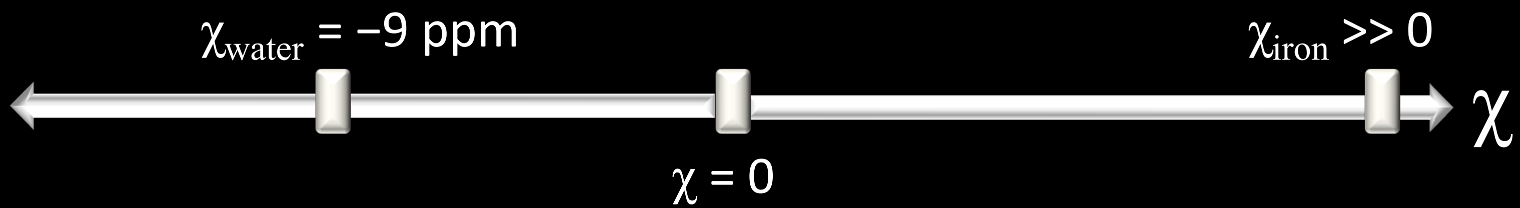

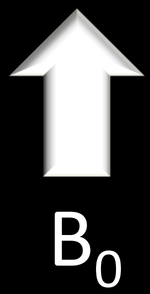

- Variations in tissue susceptibility affects the magnetic field

$\Delta\chi \rightarrow$ magnetic field perturbation

Susceptibility of Tissue

- Susceptibility χ : degree of magnetization of a material when placed in a magnetic field

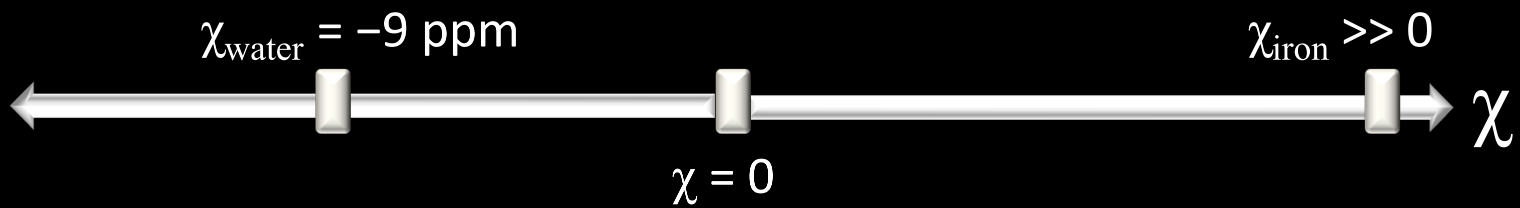

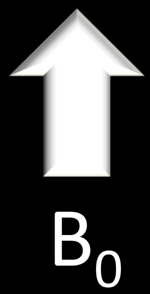

- Variations in tissue susceptibility affects the magnetic field
- Field perturbation causes a change in MR signal phase

$$\underbrace{\Delta\chi}_{\text{estimate}} \longrightarrow \text{magnetic field perturbation} \longrightarrow \underbrace{\Delta\varphi}_{\text{measured}}$$

Quantitative Susceptibility Mapping (QSM)

- Quantitative Susceptibility Mapping (QSM) aims to quantify tissue magnetic susceptibility with applications such as,
  - ❖ Tissue contrast enhancement[1]
  - ❖ Estimation of venous blood oxygenation[2]
  - ❖ Quantification of tissue iron concentration[3]

[1] Duyn JH *et al*., PNAS 2007 [2] Fan AP *et al*., ISMRM 2010 [3] Liu T *et al*., ISMRM 2010

Quantitative Susceptibility Mapping (QSM)

- Quantitative Susceptibility Mapping (QSM) aims to quantify tissue magnetic susceptibility with applications such as,
  - Tissue contrast enhancement[1]
  - Estimation of venous blood oxygenation[2]
  - Quantification of tissue iron concentration[3]
- Estimation of the susceptibility map $\boldsymbol{\chi}$ from the unwrapped phase $\boldsymbol{\varphi}$ involves solving an inverse problem,

$$\boldsymbol{\delta} = \mathbf{F}^{-1}\, \mathbf{D}\, \mathbf{F}\, \boldsymbol{\chi}$$

F: Discrete Fourier Transform

D: susceptibility kernel

$\boldsymbol{\delta} = \boldsymbol{\varphi}/(\gamma \cdot TE \cdot B_0)$: normalized field map

[1] Duyn JH *et al*., PNAS 2007 [2] Fan AP *et al*., ISMRM 2010 [3] Liu T *et al*., ISMRM 2010

Quantitative Susceptibility Mapping (QSM)

- Quantitative Susceptibility Mapping (QSM) aims to quantify tissue magnetic susceptibility with applications such as,
  - ❖ Tissue contrast enhancement[1]
  - ❖ Estimation of venous blood oxygenation[2]
  - ❖ Quantification of tissue iron concentration[3]
- Estimation of the susceptibility map χ from the unwrapped phase φ involves solving an inverse problem,

$$\delta = F^{-1} D F \chi$$

δ: measured

χ: estimate

F: Discrete Fourier Transform

D: susceptibility kernel

$\delta = \varphi/(\gamma \cdot TE \cdot B_0)$: normalized field map

[1] Duyn JH *et al*., PNAS 2007 [2] Fan AP *et al*., ISMRM 2010 [3] Liu T *et al*., ISMRM 2010

Quantitative Susceptibility Mapping (QSM)

- Quantitative Susceptibility Mapping (QSM) aims to quantify tissue magnetic susceptibility with applications such as,
  - ❖ Tissue contrast enhancement[1]
  - ❖ Estimation of venous blood oxygenation[2]
  - ❖ Quantification of tissue iron concentration[3]
- Estimation of the susceptibility map $\boldsymbol{\chi}$ from the unwrapped phase $\boldsymbol{\varphi}$ involves solving an inverse problem,

$$\boldsymbol{\delta} = \mathbf{F}^{-1}\, \mathbf{D}\, \mathbf{F}\, \boldsymbol{\chi}$$

- The inversion is made difficult by zeros in susceptibility kernel **D**

$$\mathrm{D} = \frac{1}{3} - \frac{k_z^2}{k_x^2 + k_y^2 + k_z^2}$$

|D|

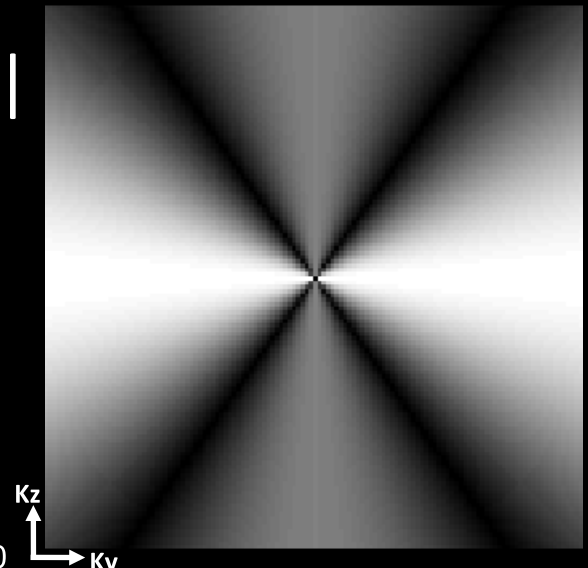

[1] Duyn JH *et al.*, PNAS 2007 [2] Fan AP *et al.*, ISMRM 2010 [3] Liu T *et al.*, ISMRM 2010

Quantitative Susceptibility Mapping (QSM)

- Quantitative Susceptibility Mapping (QSM) aims to quantify tissue magnetic susceptibility with applications such as,
  - ❖ Tissue contrast enhancement[1]
  - ❖ Estimation of venous blood oxygenation[2]
  - ❖ Quantification of tissue iron concentration[3]
- Estimation of the susceptibility map χ from the unwrapped phase φ involves solving an inverse problem,

$$\delta = F^{-1} D F \chi$$

|D|

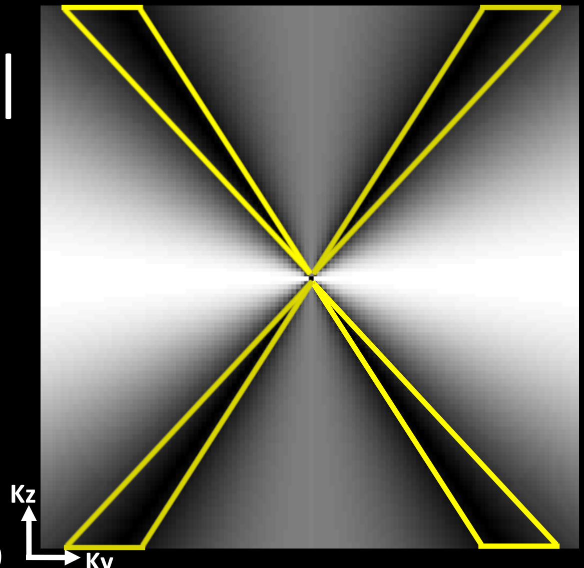

- Undersampling is due to physics
  Not in our control

[1] Duyn JH *et al*., PNAS 2007 [2] Fan AP *et al*., ISMRM 2010 [3] Liu T *et al*., ISMRM 2010

Regularized Inversion for QSM

|**D**|

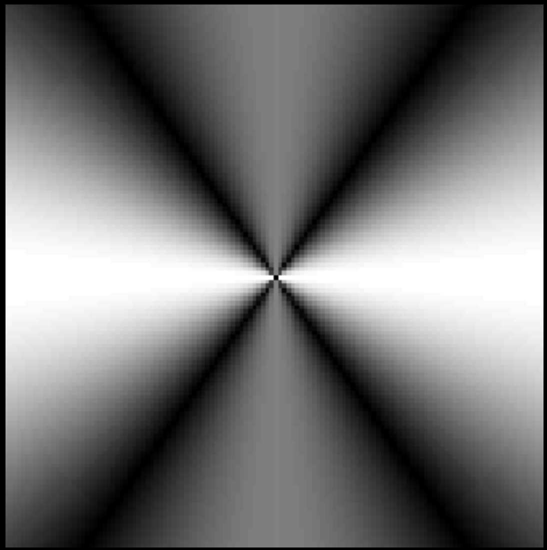

Regularized Inversion for QSM

|**D**|

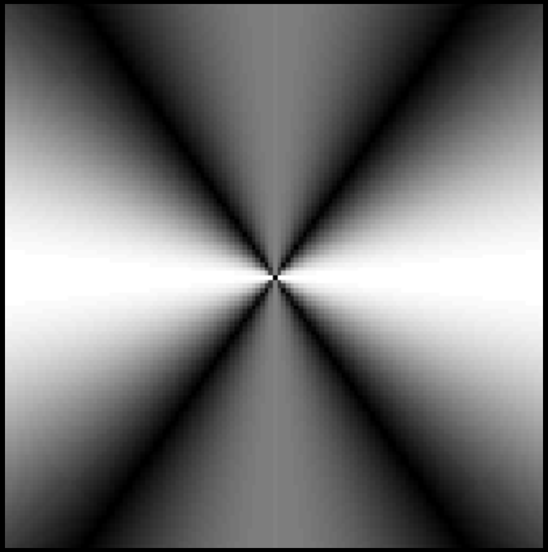

$\delta = F^{-1} D F \chi$

⬇

$\chi = F^{-1} D^{-1} F \delta$

log|**D**$^{-1}$|

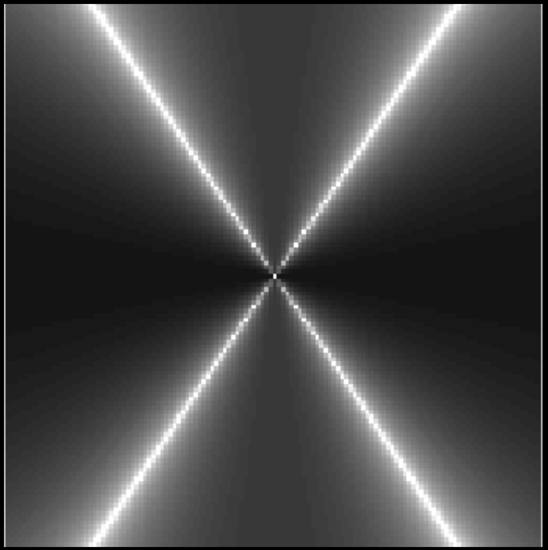

Regularized Inversion for QSM

$|\mathbf{D}|$

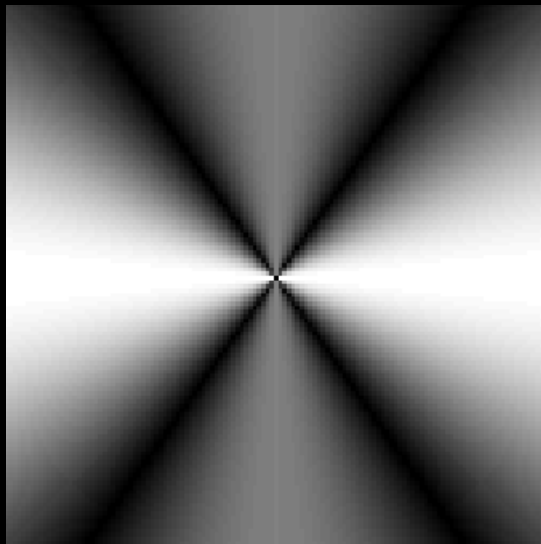

$\delta = \mathbf{F}^{-1}\,\mathbf{D}\,\mathbf{F}\,\chi$

$\Downarrow$

~~$\chi = \mathbf{F}^{-1}\,\mathbf{D}^{-1}\,\mathbf{F}\delta$~~

$\log|\mathbf{D}^{-1}|$

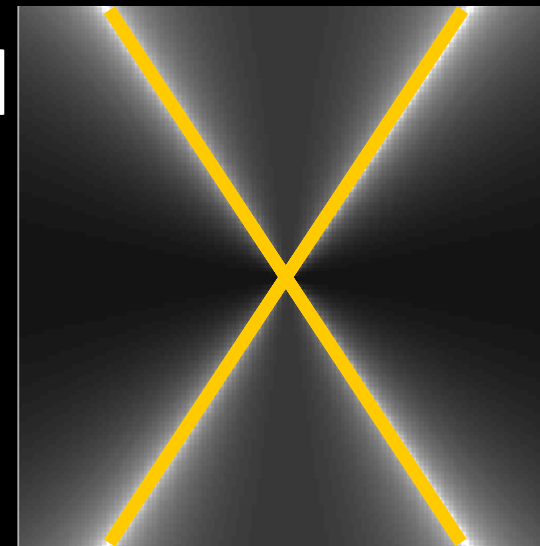

diverges to ∞

- Solving for χ by convolving with the inverse of **D** is not possible, as it diverges along the magic angle
- Use inverse problem formulation, apply regularization

Phase Processing

- Several processing steps are required to obtain the tissue phase

Phase Processing

- Several processing steps are required to obtain the tissue phase

  i. Mask out the skull

Using FSL Brain Extraction Tool[1]

[1] Smith SM, Hum. Brain Mapp. 2002

Phase Processing

- Several processing steps are required to obtain the tissue phase

  i. Mask out the skull

  ii. Unwrap the phase

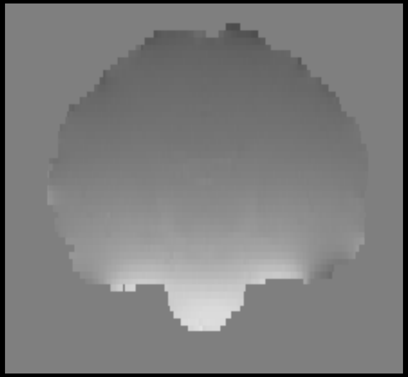

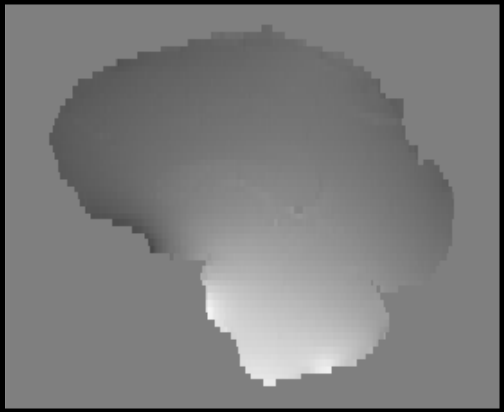

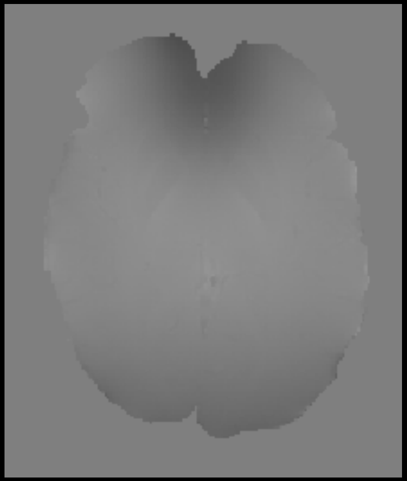

Using FSL PRELUDE[1]

[1] Jenkinson M, MRM 2003

Phase Processing

- Several processing steps are required to obtain the tissue phase

  i. Mask out the skull

  ii. Unwrap the phase

  iii. <u>Remove background phase</u>

  Phase accrued due to air-tissue interfaces needs to be removed

  This background component is ~10× larger than tissue phase

total phase

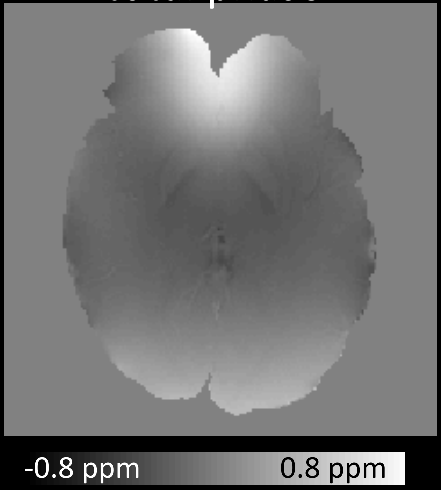

background phase[1]

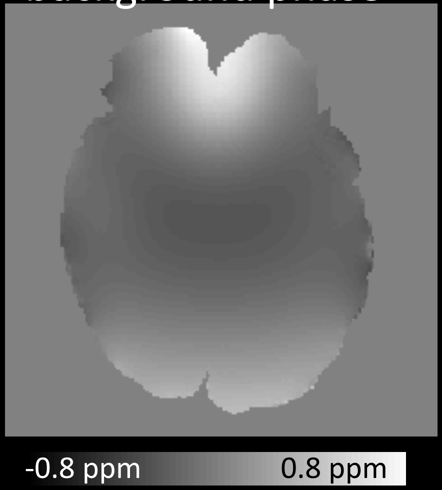

[1] Liu T, NMR in Biomedicine 2011

Phase Processing

- Several processing steps are required to obtain the tissue phase

  i. Mask out the skull

  ii. Unwrap the phase

  iii. <u>Remove background phase</u>

  Phase accrued due to air-tissue interfaces needs to be removed

  This background component is ~10× larger than tissue phase

total phase − background phase[1] = tissue phase $\boldsymbol{\delta}$

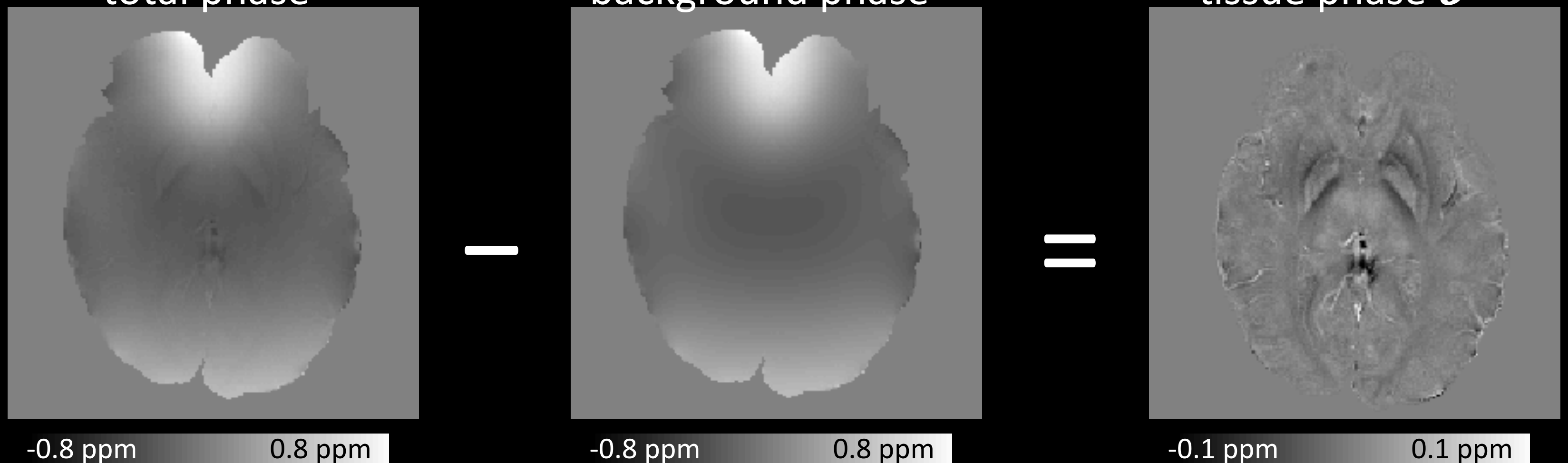

Phase Processing

- Several processing steps are required to obtain the tissue phase

  i. Mask out the skull
  ii. Unwrap the phase

  iii. Remove background phase

  Phase accrued due to air-tissue interfaces needs to be removed

  This background component is ~10× larger than tissue phase

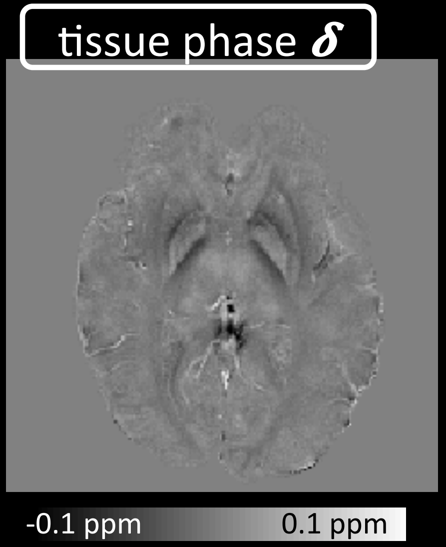

- Now we can solve for χ from tissue phase δ

$$\delta = F^{-1} D F \chi$$

L2 Regularized Susceptibility Inversion

- We seek the susceptibility map that matches the observed tissue phase,

$$\text{Find } \boldsymbol{\chi} \text{ such that } \quad \boldsymbol{\delta} = \mathbf{F}^{-1}\,\mathbf{D}\,\mathbf{F}\,\boldsymbol{\chi}$$

- **Prior:** Susceptibility is tied to the magnetic properties of the underlying tissue; hence it should vary smoothly within anatomical boundaries.

L2 Regularized Susceptibility Inversion

- We seek the susceptibility map that matches the observed tissue phase,

$$\text{Find } \boldsymbol{\chi} \text{ such that } \quad \boldsymbol{\delta} = \mathbf{F}^{-1}\, \mathbf{D}\, \mathbf{F}\, \boldsymbol{\chi}$$

- **Prior:** Susceptibility is tied to the magnetic properties of the underlying tissue; hence it should vary smoothly within anatomical boundaries.

- Employ regularization that encourages smoothness within tissues, but avoids smoothing across boundaries.

L2 Regularized Susceptibility Inversion

- We solve for the susceptibility distribution with a convex program,

$$\min \underbrace{\left\| F^{-1} D F \chi - \delta \right\|_2^2}_{\text{Data consistency}} + \lambda \cdot \underbrace{\left\| M G \chi \right\|_2^2}_{\text{Regularizer}}$$

L2 Regularized Susceptibility Inversion

- We solve for the susceptibility distribution with a convex program,

$$\min \left\| \mathrm{F}^{-1}\mathrm{D}\mathrm{F}\,\chi - \delta \right\|_2^2 + \lambda \cdot \left\| \mathrm{M}\mathrm{G}\,\chi \right\|_2^2$$

G : Spatial gradient operator in 3D

M : Binary mask derived from magnitude image, prevents smoothing across edges

λ : Determines the amount of smoothness

L2 Regularized Susceptibility Inversion

- We solve for the susceptibility distribution with a convex program,

$$\min \left\| \mathrm{F}^{-1}\mathrm{D}\mathrm{F}\,\chi - \delta \right\|_2^2 + \lambda \cdot \left\| \mathrm{M}\mathrm{G}\,\chi \right\|_2^2$$

Optimizer given by the solution of:

$$(\mathrm{F}^{-1}\mathrm{D}^2\mathrm{F} + \lambda \cdot \mathrm{G}^T\mathrm{M}\mathrm{G})\chi = \mathrm{F}^{-1}\mathrm{D}^T\mathrm{F}\,\delta$$

Large linear system, solve iteratively with Conjugate Gradient

L2 Regularized Susceptibility Inversion

- We solve for the susceptibility distribution with a convex program,

$$\min \left\| F^{-1} D F \chi - \delta \right\|_2^2 + \lambda \cdot \left\| M G \chi \right\|_2^2$$

Optimizer given by the solution of:

$$(F^{-1} D^2 F + \lambda \cdot G^T M G)\chi = F^{-1} D^T F \delta$$

Without magnitude weighting (M=Identity), we proposed a closed-form solution:

$$\chi = \underbrace{(F^{-1} D^2 F + \lambda \cdot G^2)^{-1}}_{\text{Fast inversion with two DFTs}^1} \cdot F^{-1} D^T F \delta$$

Fast inversion
with two DFTs[1]

[1] Bilgic B, JMRI 2013

L2 Regularized Susceptibility Inversion

- We solve for the susceptibility distribution with a convex program,

$$\min \left\| F^{-1} D F \chi - \delta \right\|_2^2 + \lambda \cdot \left\| M G \chi \right\|_2^2$$

Optimizer given by the solution of:

$$(F^{-1} D^2 F + \lambda \cdot G^T M G)\chi = F^{-1} D^T F \delta$$

Without magnitude weighting (M=Identity), we proposed a closed-form solution[1].

Using this inverse as **preconditioner** for Conjugate Gradient, we proposed a fast solution to the problem with magnitude weighting[2]

This improved computation speed **15-fold** relative to existing solvers

[1] Bilgic B, JMRI 2013 [2] Bilgic B, MRM 2013

Wave-CAIPI accelerated QSM

- Wave-CAIPI enabled 3D GRE allows rapid QSM acquisition

- Compare in vivo phase and QSM from
  Wave-CAIPI, 2D-CAIPI and Bunch Phase Encoding:
  - At 3T and 7T
  - R = 3x3 acceleration, scan time = 2.3 min
  - 1 mm isotropic resolution
  - TE = 20 ms, TR = 40 ms
  - 240x240x120 FOV

Wave-CAIPI accelerated QSM

- Wave-CAIPI enabled 3D GRE allows rapid QSM acquisition

- Compare in vivo phase and QSM from Wave-CAIPI, 2D-CAIPI and Bunch Phase Encoding

- Phase Processing:
  - Laplacian unwrapping[1] and
  - SHARP filtering for background removal[2]

  } **14 seconds**

- Susceptibility Inversion:
  - Fast L2-regularized inversion[3]

  } **32 seconds**

[1] Li W, NIMG 2011 [2] Schweser F, NIMG 2011 [3] Bilgic B, MRM 2013

3 Tesla, R=3x3, 1 mm iso, 2.3 min acq

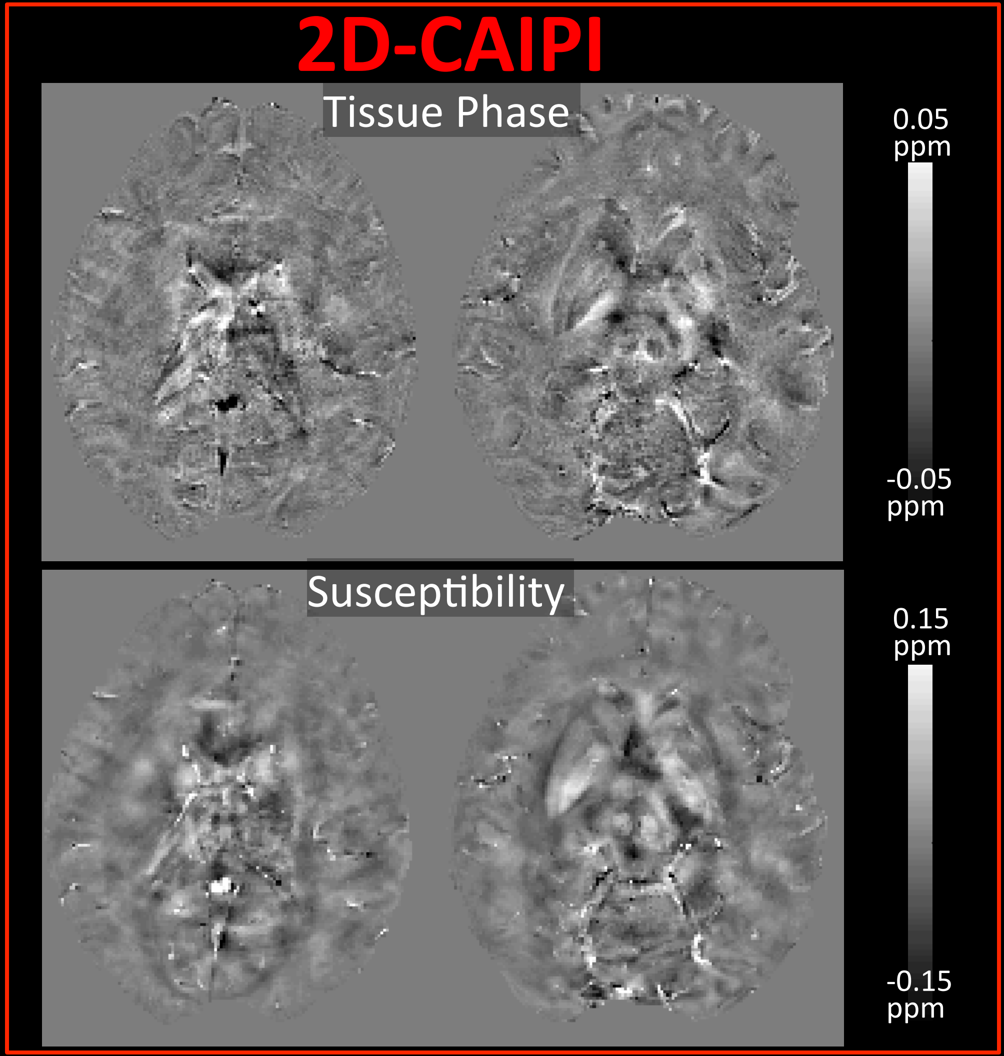

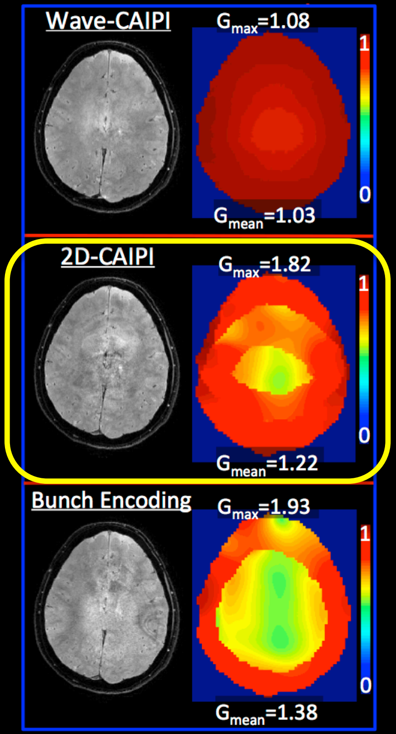

3 Tesla, R=3x3, 1 mm iso, 2.3 min acq

Bunch Encoding

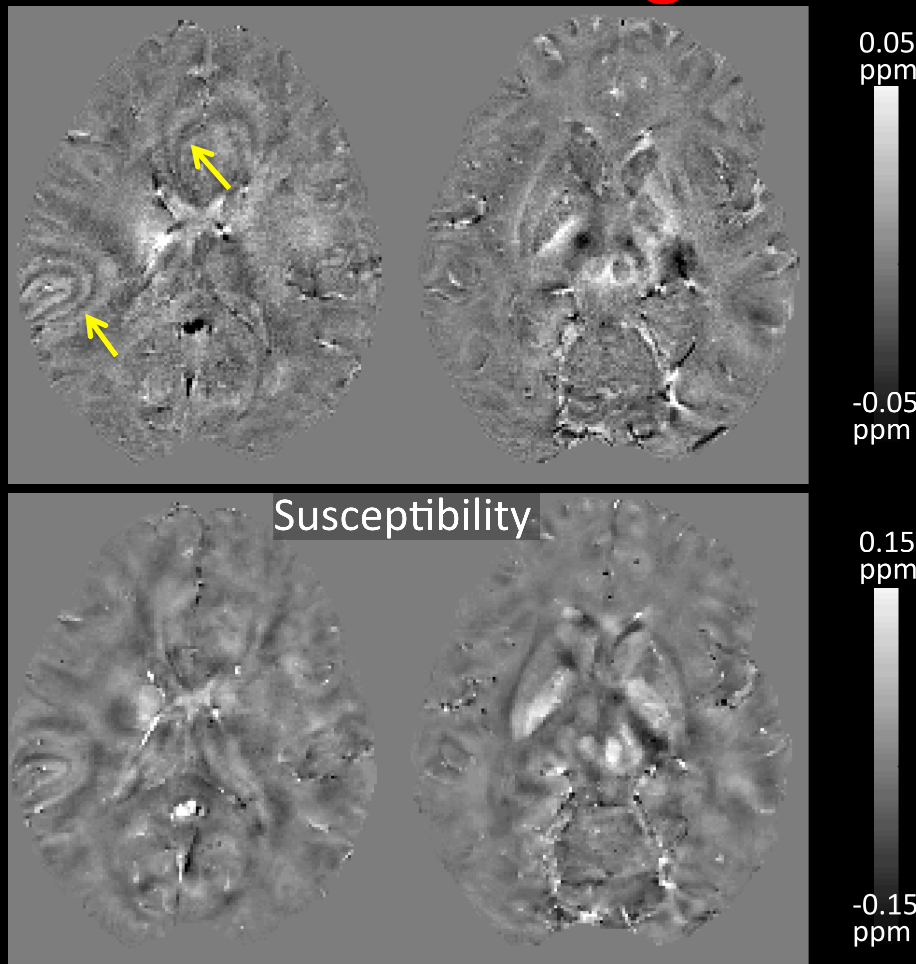

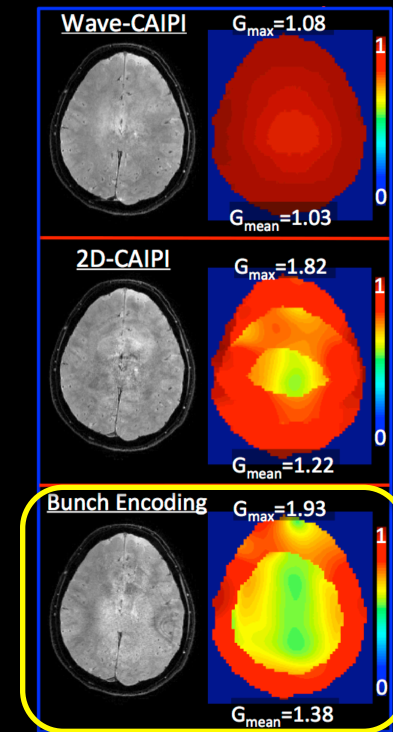

3 Tesla, R=3x3, 1 mm iso, 2.3 min acq

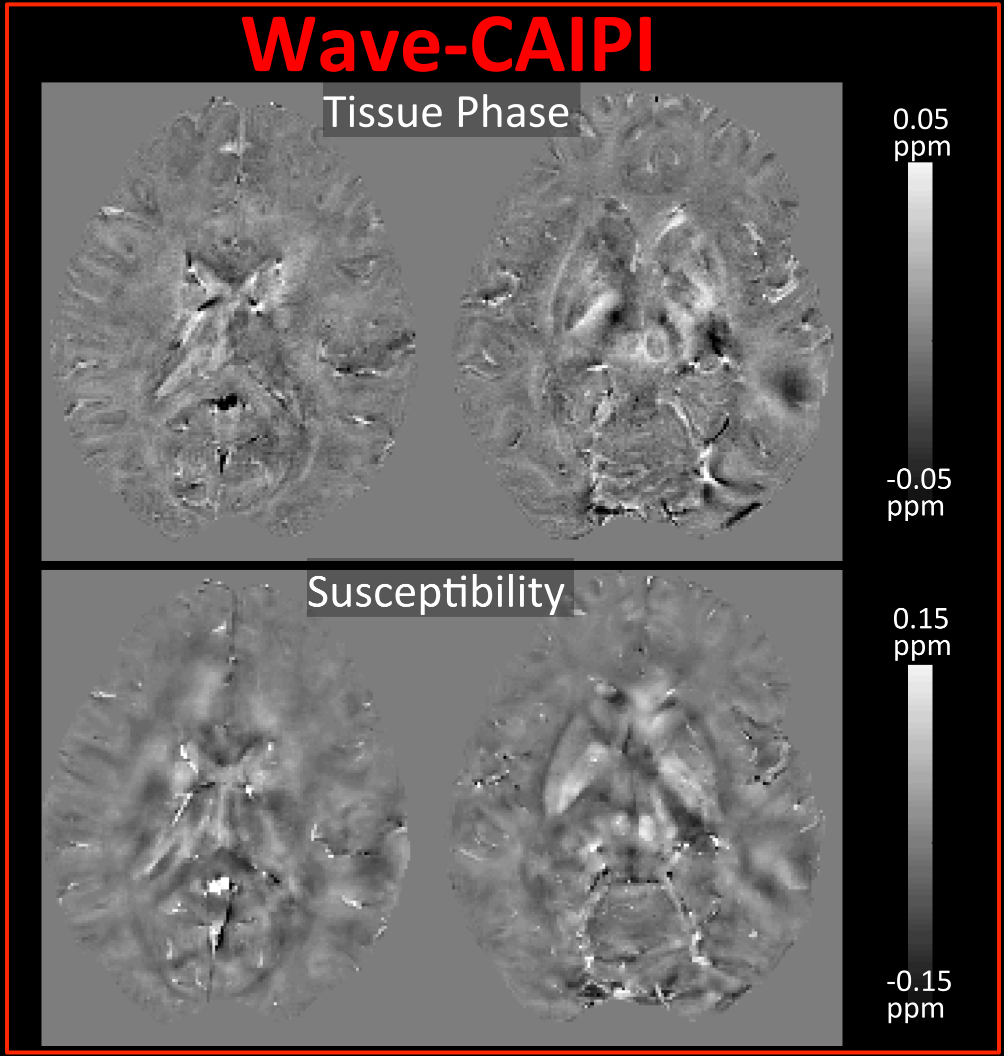

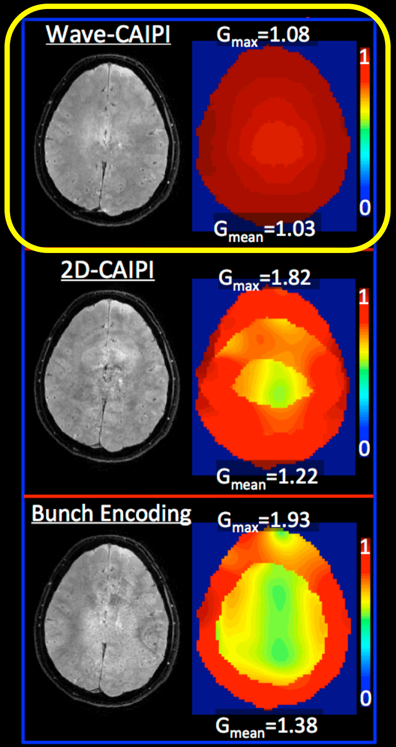

7 Tesla, R=3x3, 1 mm iso, 2.3 min acq

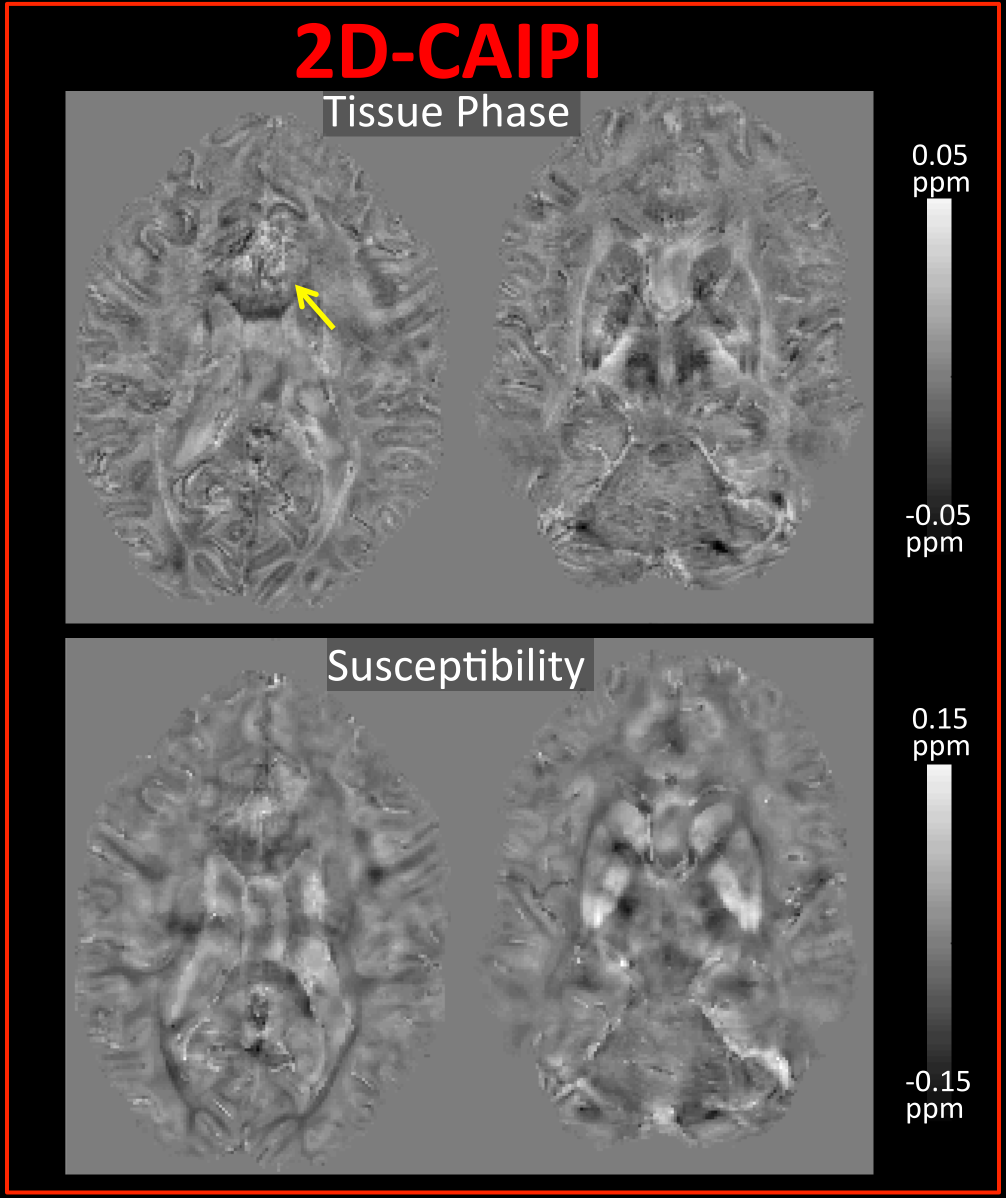

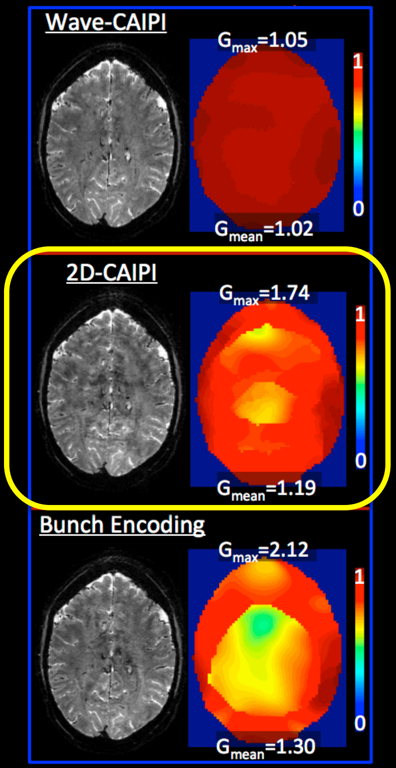

7 Tesla, R=3x3, 1 mm iso, 2.3 min acq

Bunch Phase

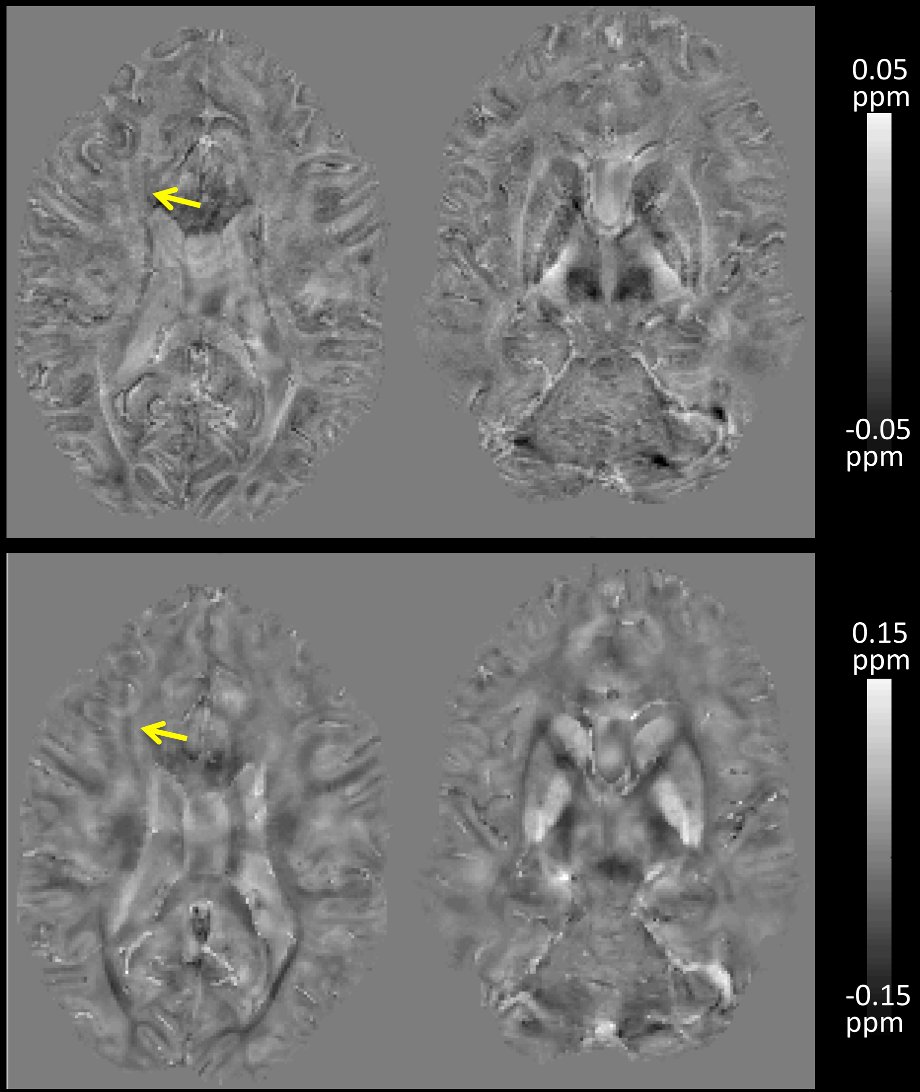

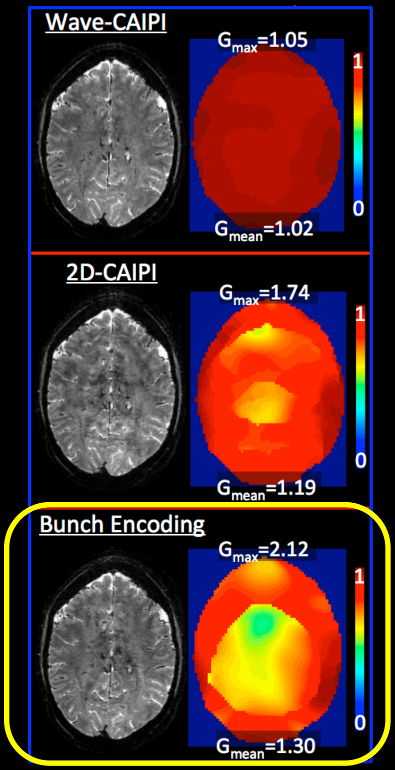

7 Tesla, R=3x3, 1 mm iso, 2.3 min acq

Wave-CAIPI

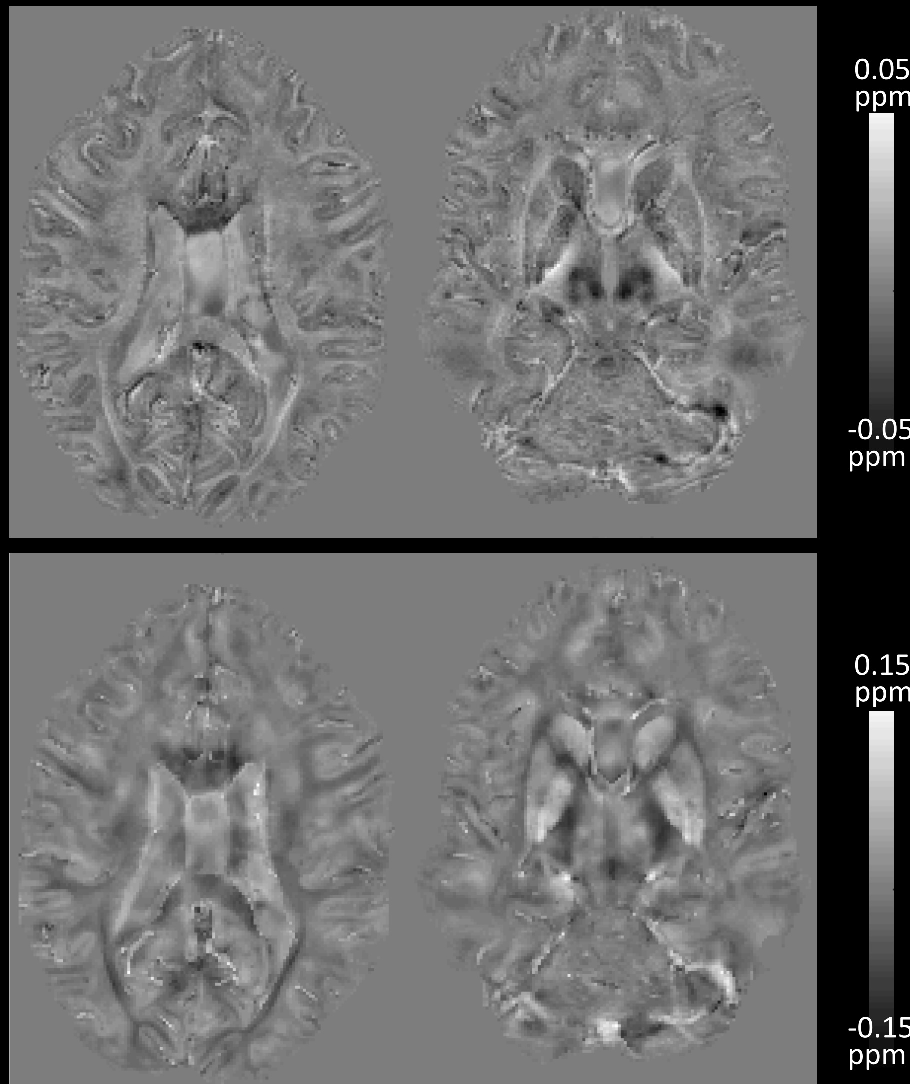

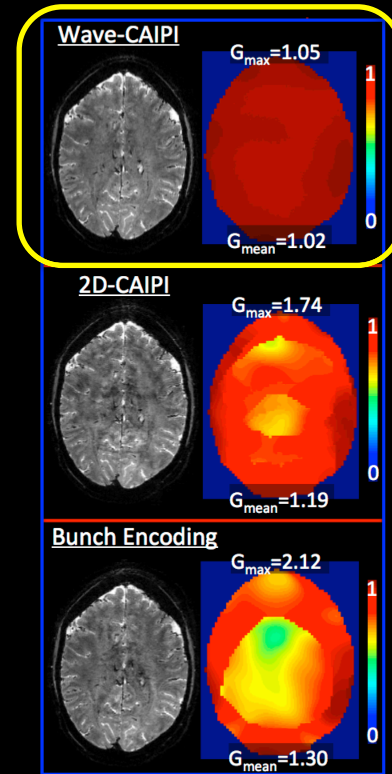

Summary

- Propose Wave-CAIPI acquisition/reconstruction scheme for highly accelerated 3D imaging
- Wave-CAIPI offers 2-fold improvement in g-factor and image artifact penalties compared to 2D-CAIPI and Bunch Phase Encoding

Summary

- Propose Wave-CAIPI acquisition/reconstruction scheme for highly accelerated 3D imaging
- Wave-CAIPI offers 2-fold improvement in g-factor and image artifact penalties compared to 2D-CAIPI and Bunch Phase Encoding
- Deployed in GRE imaging, Wave-CAIPI allows 9-fold acceleration with ~perfect SNR retention at 3T and 7T
- Combined with fast phase and susceptibility processing methods, it enables QSM at 1 mm resolution in 2.3 min

Thank you for your attention